A Major-II Project Report

on

3D Modelling and Finite Element Analysis of Knee Joint Using Computed Tomography (CT) Data

submitted in partial fulfilment for the award of the degree

of

Masters of Technology

in

Mechanical Engineering

with specialisation in

Computational Design

by

Abid Hussain
(2K13/CDN/01)

under the guidance

of

Dr. R.C. Singh
(Assistant Professor)

Department of Mechanical Engineering

Delhi Technological University, Delhi

2014-15

Certificate

This is to certify that the Major-II Project Report entitled "3D Modelling and Finite Element Analysis of Knee Joint Using Computed Tomography (CT) Data " is a bonafide work carried out by Mr. Abid Hussain (2K13/CDN/01) of M.Tech (Computational Design) and submitted to Department of Mechanical Engineering, Delhi Technological University, Bawana Road, Delhi in partial fulfilment of the requirement for the award of the Degree of the Masters of Technology under specialization in Computational Design under our supervision. It is further certified that the embodied work has not been submitted to any other institution for the award of other degree or certificate.

Dr. R.C Singh
Assistant Professor
Department of Mechanical Engg
Delhi Technological University

DECLARATION

I, Abid Hussain, hereby declare that this submission is my own work and that, to the best of my knowledge and belief, it contains no material previously published or written by another neither person nor material which to a substantial extent has been accepted for the award of any other degree or diploma of the university or other institute of higher learning except where do acknowledgement and references has made in the text.

Abid Hussain
M.Tech II Year
2K13/CDN/01
Department of Mechanical Engg.
Delhi Technological University

ABSTRACT

Knee joint consists of different components, tibia, femur, patella, ligaments, menisci and tendons. They make it one of the most complicated structures, experiencing different critical loads in human body along with movement, locomotion and performing physical activities. Present study focuses on the analysis of maximum principal stress, Maximum principal elastic strain and total deformation on knee joint when for various loads applied on it with different boundary conditions. The idea is to first of all present a graphical modeling methodology of human anatomical constructs like the bones, the tibia, the femur and the patella. Secondly, it involves performing a FE analysis of the human knee joint under static loading conditions. The 3-D CAD model of the human knee joint is generated by the use of CT images transformed into geometric model with the help of Simpleware ScanIP. The models are then imported to ANSYS 15.0 to obtain the results of the stress magnitude by finite element analysis. A study of load range of 540N to 790 N at standing position and at flexion angle of 90^0 is carried out. The mechanical properties like Poisson's Ratio and Young's Modulus of the human bones differ from individual to individual, usually according to age, weight and gender. The most important purpose of FEA (Finite Element Analysis) in orthopedic biomechanics is to predict and understand the mechanical nature of bones, develop design of implants with improvement, and eliminate/minimize the cost and time required in vivo and in vitro experimentation. Finite Element modeling is also used for bone remodeling and healing phenomena of conventional and biomimetic devices, such as hip replacements. Of late, computational modeling along with bone biology, biochemistry, and thermodynamics is being used to create new therapeutic strategies related to bone loss and other bone related diseases. The study helps in the design of implant by giving emphasis on different types of material to be used depending upon the amount of stress experienced at different locations in knee joint. Overall, the study provides a relation in the stress magnitude in different components of knee joint and will be helpful in providing a guideline for fabrication of prosthetic implant in the line of intimation with reduced number of experiments so that implants with better stress management and enhanced load bearing capacity can be designed.

ACKNOWLEDGEMENTS

First and foremost, I would like to thank the Almighty God for giving me the strength and wisdom to carry out this work.

I would also like to express my sincere gratitude to my supervisor, Dr. R C Singh, Professor, Delhi Technological University, New Delhi, for his continuous support, creativity, his excellent skill, patience, motivation, enthusiasm, and immense knowledge which have always been a constant source of motivation for me. His excellent guidance, perseverance, invaluable suggestions made this work possible and complete.

My profound gratitude to Prof R. S. Mishra, Head of Mechanical Department, Delhi Technological University, New Delhi, for providing effective management, necessary facilities and valuable suggestions for success of this work.

I humbly pay my sincere thanks to the entire fraternity of Mechanical Department, Delhi Technological University, New Delhi, for their kind cooperation throughout the project work.

I owe my success to my loving parents for their abundant blessings and unconditional support and my siblings for being my source of strength throughout my life.

Last but not the least, I would like to express my heartfelt gratitude to all my friends and well-wishers without whose support and best wishes it could not have been possible to complete a task of this magnitude.

Abid Hussain

TABLE OF CONTENTS

LIST OF FIGURES

LIST OF TABLES

LIST OF ABBREVIATIONS

1. ACL- Anterior Cruciate Ligament
2. BMI- Body Mass Index
3. CAD- Computer Aided Design
4. CES- Cambridge Engineering Selector
5. CT- Computed Tomography
6. FEA- Finite Element Analysis
7. FBD- Free Body Diagram
8. GRF- Ground Reaction Force
9. LCL- Lateral Collateral Ligament
10. MCL- Medial Collateral Ligament
11. NURBS- Non-Uniform B-Splines
12. OA- Osteoarthritis
13. PCL- Posterior Cruciate Ligament
14. STL- Stereo Lithography
15. TKA- Total Knee Arthroplasty
16. TKR- Total Knee Replacement

Chapter 1

INTRODUCTION

One of the most complex joints in the human body is the knee joint. The knee joint consists of various components, that includes tibia, femur, patella, ligaments, menisci and tendons that make it complex in structure. It is also the most load-bearing joint [1].To perform the function of stabilizing the knee from front as well as from the back during normal activities and also during rigorous athletic activities there is both an anterior cruciate ligament (ACL) and a posterior cruciate ligament (PCL). The motion of the joint depends, to great extent, on the function of the soft tissue constituents. This includes - posterior and anterior cruciate ligaments (PCL and ACL, respectively), and medial and lateral collateral ligaments (MCL and LCL, respectively). The the tibiofemoral joint constitutes these four ligaments. These ligaments allow primarily flexion/extension and rotation of the joint by enabling the bony constituents (femur and tibia) to translate and rotate relative to each other. Articular cartilage covers the weight bearing surfaces of knees. The medial and lateral meniscus act as shock absorbers and help to center the knee joint during activity. They also minimize the amount of stress on the articular cartilage. Due to the geometric complexity and non-linearity of the materials of the knee, it is difficult to analyze the mechanical behavior of the knee joint.

Several factors like increasing age and injuries and many pathological disorders lead to the weakening of bone and muscles. This leads to wear the joint, resulting in the development of Osteoarthritis. This causes deformity, stiffness, pain and swelling in the knee joint, as a result, causing the cumulative failure of joint functions [2]**.** One of the most commonly accepted solutions of this problem is the total knee replacement (TKR) or total knee Arthroplasty (TKA) [3]. This is a surgical procedure in which artificial knee components are used to replace the damaged or osteoarthritic surfaces of bone [4]. This procedure involves significant risk factors for failure of the total knee Arthroplasty. Risk factors include: age and gender of the patient, improper alignment of femur and tibia bone, type of implant, diagnosis, type of fixation, and design of the patellar component. It is important that the design of the patellar component is proper as it plays an important role in longevity and success of TKA. In TKA validation, the

design of knee implant systems is validated properly by understanding the mechanics of the restored knee and optimizing the design in order to more closely replicate the healthy knee.

The present study focuses on the analysis of stress magnitude on knee joint when introduced with different loads acting upon it with varying the inclination angles. The first topic is to present a graphical modeling approach of human anatomical structures of the bones namely the femur, the tibia and the patella. The second theme involves making a finite element analysis of knee joint under static loading conditions. CT scan image data of lower extremity of a patient is obtained and image processing is carried out to segment the femur and tibia bone. The 3-D CAD model of the knee joint is designed by using CT Images converted into geometric model using Simpleware ScanIP 7.0. ANSYS 15.0 is then used for analysis to get the particular results of stress levels using finite element analysis. The study is carried out for a load of range 540N to 790 N and during standing position of the knee. The mechanical properties like Poisson's Ratio and Young's Modulus of the bones vary in human from person to person, in general according to age, weight and gender. The study helps in the design of implant by giving emphasis on different types of material to be used depending upon the amount of stress experienced at different locations in the knee joint. The study, in general, presents a relation in the stress magnitude in different components of knee joint and will be helpful in providing a guideline for fabrication of prosthetic implant in the line of intimation with reduced number of experiments so that implants with better stress management and enhanced load bearing capacity can be designed. By performing these simulations a better perception will be achieved in viewing the stress levels and how they are distributed on the articulating surfaces.

1.2 RESEARCH OBJECTIVE:

To help in the design of implant: Success of TKR depend on a number of factors which include age and gender of the patient, improper alignment of femur and tibia bone, type of implant, diagnosis, type of fixation, and design of the patellar component. It is important that the design of the patellar component is proper as it plays an important role in success and longevity of TKA. By giving emphasis on different types of material to be used depending upon the amount

of stress experienced at different locations in knee joint the design of the implant can be greatly improved.

Overall, the study presents a relation in the stress magnitude in different components of knee joint and will be helpful in ***providing a guideline for fabrication of prosthetic implant in the line of intimation with reduced number of experiments so that implants with better stress management and enhanced load bearing capacity can be designed***.

CHAPTER 2

LITERATURE REVIEW

This section covers the anatomy of human knee and Total Knee Arthroplasty. A first, the anatomy of the knee will be discussed. The interaction of different components constructing the knee and the roles played by them has been explained. This will be followed by an overview of Osteoarthritis and Total Knee Arthroplasty, explaining the disease and the means to deal with it. Lastly, an illustration of the effects of different stress in the knee is given by examining the effect of weight transfer through the lower extremity.

Anatomy of the Knee Joint

In the human body, the knee joint is one of the most complicated joints. It is also the largest joint of the human body. It comprises of four bones – femur, patella, tibia and fibula, and the tendons, which connect the knee bones to the leg muscles that help in the movement of knee joint, and, the ligaments, which join the bones and provide stability to the knee.

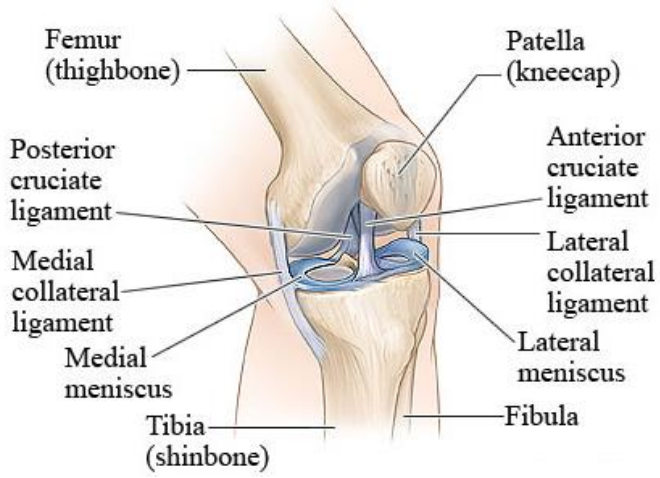

Figure 1 Anatomy of the Knee Joint (www.webmd.com)

The knee joint is made up of the combination of the four bones (Figure 1). Knee joint is one of the most troubled joints in a nimble human body because the knee is under extreme stress with so many activities [10]. Stability of the knee joint depends, primarily, the joint capsule, on the ligaments and the muscles around the joint. Predominantly, the function of the knee is to provide flexibility in movement and stability in weight tolerance; although, it is particularly unstable medially and laterally.

The distal edge of the femur constitutes the convex medial and lateral condyles that connect with the tibia and the patella. Compared to the surface of the lateral condyle, the articular surface of the medial condyle is elongated from front to back. A hollowed femoral groove or trochlea is formed by the two condyles to receive the patella at the anterior. The tibial plateau, which is the proximal end of the tibia, connects with the condyles of the femur (Figure 2).

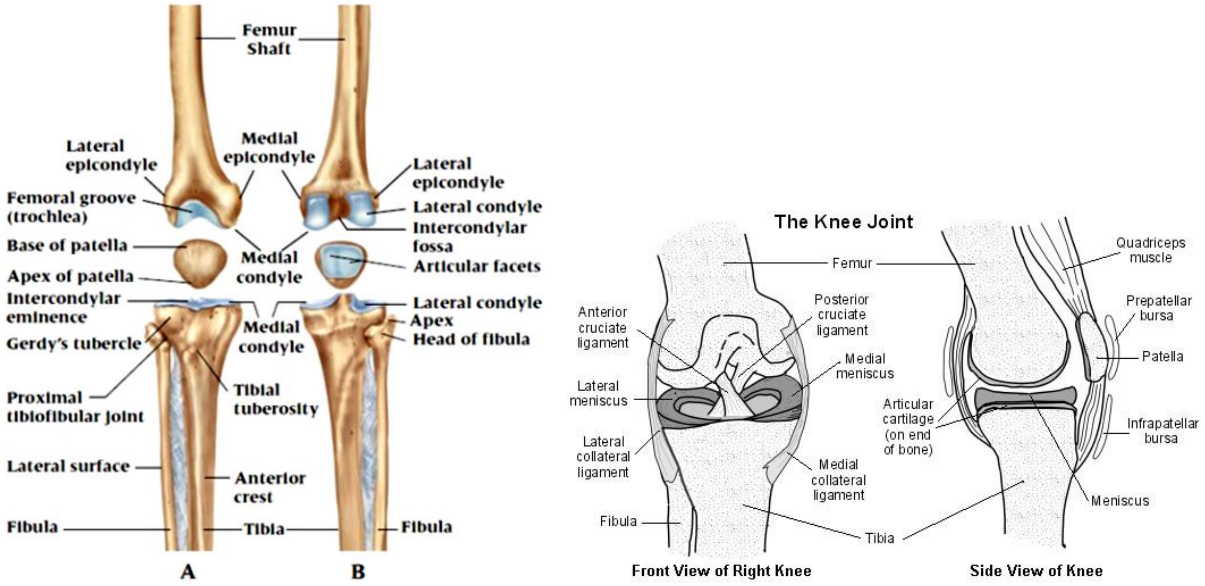

Figure 2 Bones of knee joint. A. anterior view B. posterior view **Figure -** www.patient.co.uk

The condyles of the femur and tibia, which is the articular surface of the knee, is covered by hyaline cartilage. The cavity between these articular cartilages is filled with menisci. The two oval (semilunar) fibrocartilages are menisci (Figure 3). Its major functions are to cushion any stresses placed on the knee joint, deepen the articular facets of the tibia, and maintain spacing

between the femoral condyles and tibial plateau [11] [12]**.** When the knee is bent at 90°, the menisci, mainly the medial meniscus, help to stabilize the knee [13].

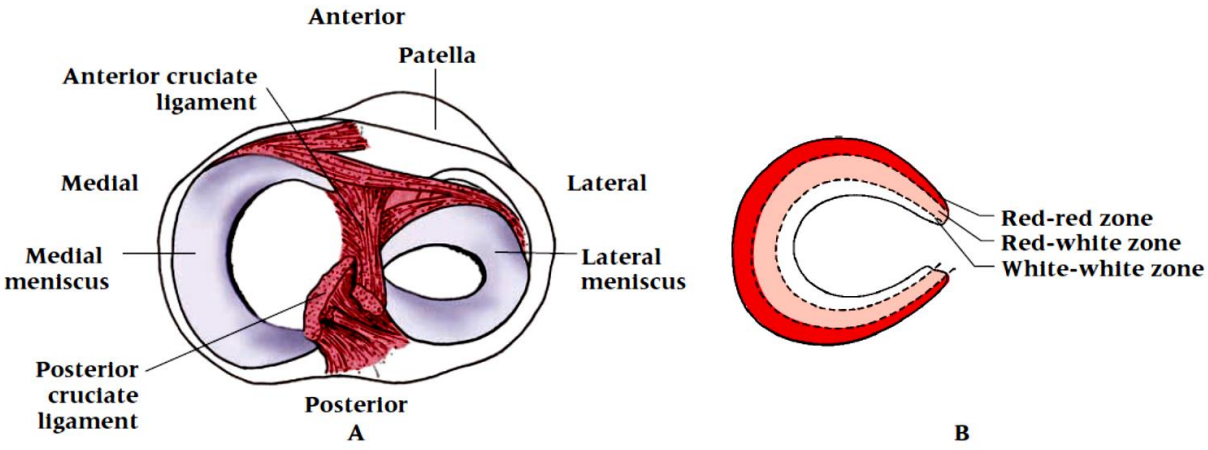

Figure 3 A. Menisci and blood supply of the knee, B. Three vascular zones.

The knee movement is regulated by the shape of the articulating surfaces and its four ligaments [14] including the collateral ligaments, the cruciate ligaments, and the capsular ligaments (Figure 4).

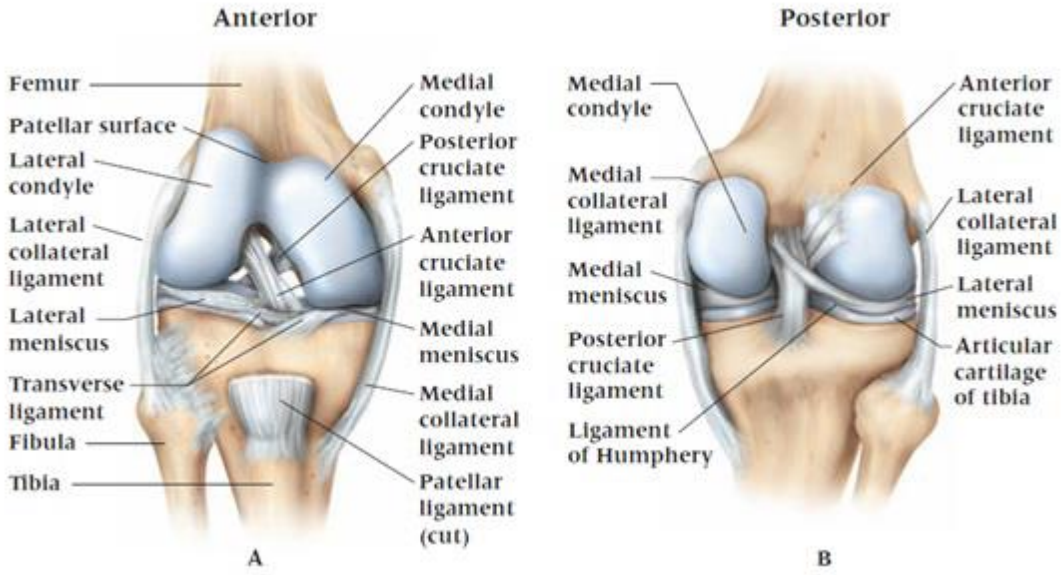

Figure 4 Ligaments of the knee A. Anterior view, B. Posterior view.

Knee stability depends substantially on the cruciate ligaments [15]. The medial collateral ligament (MCL) and the lateral collateral ligament (LCL) are present at the sides of the joint.

They serve as stabilizers for the side-to-side stability of the joint. The MCL is made up of two ligament structures, the deep component and superficial component. The MCL is a broader ligament. The LCL compared to the MLC, is a separate cord-like structure. The anterior cruciate ligament (ACL) is at the center of the joint, on its front. ACL acts as a stabilizer of the femur on the tibia. It serves to prevent the tibia from rotating and sliding forward during jumping, agility and slowing down activities. The posterior cruciate ligament (PCL) is placed directly behind the ACL to prevent the tibia from skidding to the rear.

The ligaments prevent excessive anterior and posterior sliding of the femur on the tibia during flexion and load application [16]. They also reduce internal rotation of the femur on the tibia. The four ligaments work as a 4-bar linkage system providing 6-degrees of freedom: 3 rotational (flexion/extension, internal/external and varus/valgus) and 3 translation (anterior/posterior, medial/lateral and inferior/superior) [16].

Osteoarthritis in Knee

One of the most commonly affected joints is the knee joint and the most common type of joint disease is Osteoarthritis (OA). Bone joints are affected in Osteoarthritis. The affected joint does not move as smoothly as it should because the surfaces within the joints are damaged (Figure 5). This condition is known as Osteoarthrosis, arthrosis, degenerative joint disease or wear and tear. Although the main cause of this disease is not known yet, but it grows due to several factors. It is more often because of either age (above 40 years) or gender or obesity or joint injury or a combination of any of these factors. These factors lead to the condition in which some of the cartilage covering at the end of the bones slowly starts to become coarse and thin. This can happen in the cartilage under the kneecap and on the surface of the knee joint. As a reaction to this the bone underneath the cartilage becomes thicker and broader. The tissues within the joint become more active than usual – in a way the body is tries to repair the damage.

- At the edges the bone grows outwards. They form bony spurs called osteophytes. This affects the thigh bone, kneecap or the shin bone.
- The joint may swell due to the extra fluid produced by the synovium swelling. This phenomenon is called called an effusion or water on the knee.
- The ligaments and capsule slowly contract and thicken in a way to stabilize the joint.

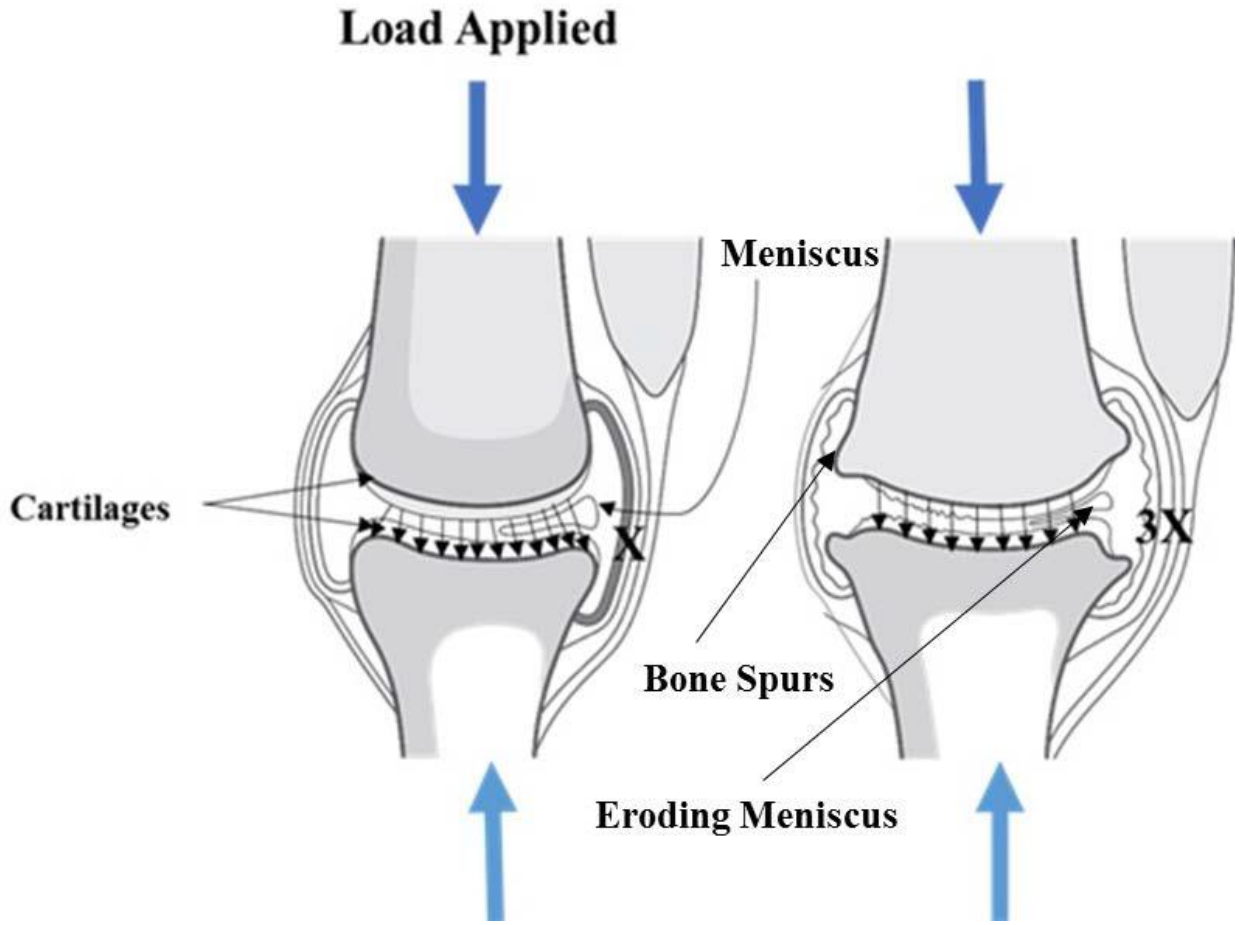

Figure 5- An illustration of how loss of the meniscus creates pressure points on the articulating surfaces.

Self-repair does not always work. In other cases the knee gets damaged. The symptoms may become worse and persistent with time due to the instability of the joint and increase in the weight being put onto the other parts of the joint.

Along with this, the meniscus, which acts as a pressure distributor over the articulating surfaces, is vanished and pressure points are created. These pressure points lead to the wear of the articular cartilage. This loss of articular cartilage in turn exposes the bone of the articulating surfaces resulting in pain on stress and movement (Figure 5) [17].

Total Knee Replacement (TKA)/ Total Knee Arthroplasty (TKR)

Osteoarthritis can be cured by Total Knee Replacement (TKA) or Total Knee Arthroplasty (TKR). TKA is a surgical procedure in which the worn out, damaged, or diseased surfaces of a knee joint is removed and replaced with artificial components (Figure 7) [18]. The distal femur and the proximal tibia are removed and replaced by metal shells in TKA (Figure 6).

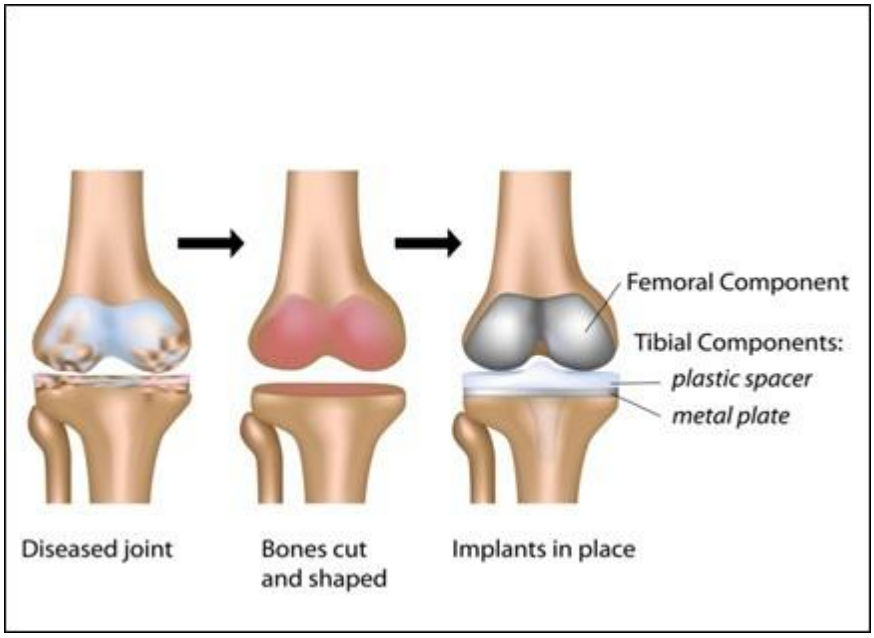

Figure 6 Illustration of removal of degraded surfaces for Total knee replacement (from http://fxrxinc.com)

Arthritic portion of thigh bone is replaced by femoral component after removal of damaged surfaces, arthritic portion of shin bone is replaced by tibial component which is done using bone cement, and cartilage is replaced by tibial insert which acts as shock absorber. Tibial insert is made of ultra-high molecular weight polyethylene (UHMWPE). Knee cap is replaced by patellar component (Figure 8) [16].

Figure 7 Components of Total Knee Arthroplasty (from http://prospektmarch.blogspot.in)

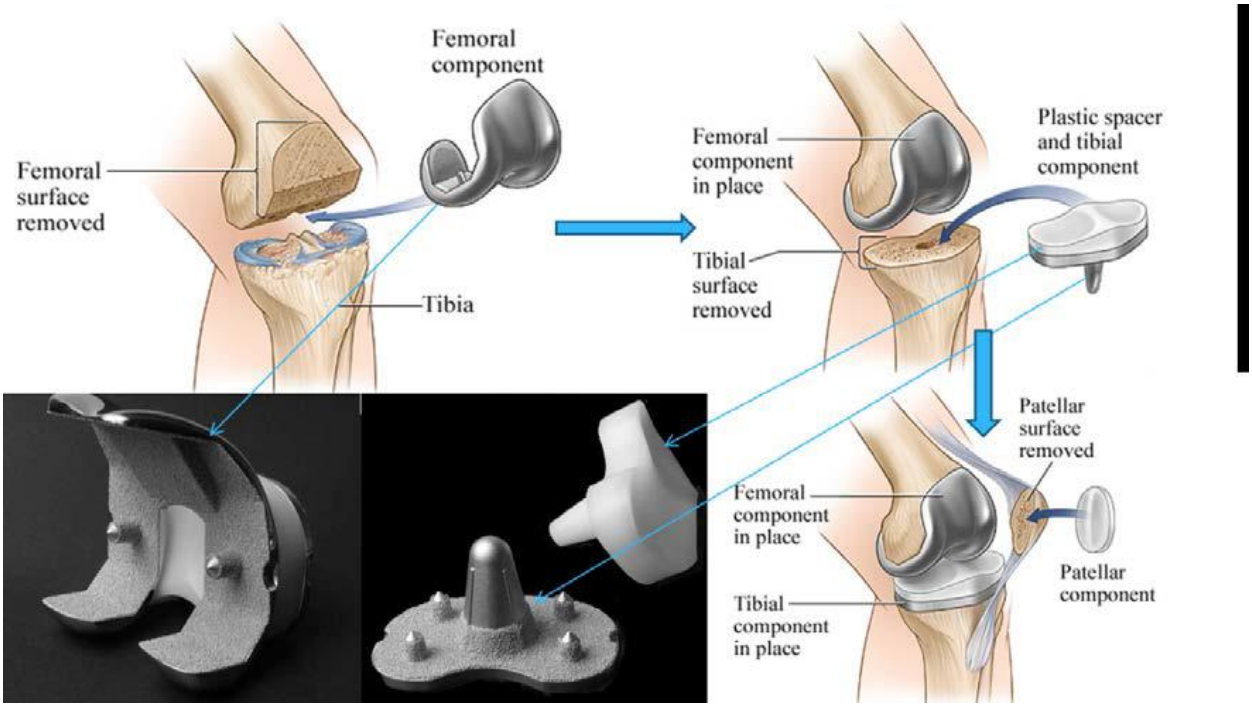

Figure 8 Representation of TKR steps (from http://www.healthline.com)

3D active contour segmentation of anatomical structures (Femur & Tibia) from CT Images

An initial evaluation of the accuracy of 3D models generated from one segmentation software technique was provided by Eric et al [30]. The main purpose of this study was to assess the

accuracy of 3D bone and cartilage models by using image acquisition, segmentation and reconstruction tools commonly used in biomedical research. The study of cadaveric knees which involved insertion of screws in bones was done. The results illustrated that bone surfaces modelled from manually segmented CT scans were significantly accurate.

Using MR for cartilage surface model segmentation is less preferred since it tends to over-estimate the thickness of cartilage by 1.15 mm for both femur and tibia. Computed Tomography (CT) images use a variational approach for segmenting bone structures and was presented by Jeff et al [31]. A new function in the field of image segmentations was introduced, and further minimized to a gradient descent partial differential equation. The results determined that the function provided similarity of the intensity characteristics of the bone and tissue regions based on the similarity of their respective cumulative distribution functions. The approach was validated by comparing the results of the tests on several CT databases with the ground truth segmentations.

Ravikant et al. on three-dimensional modeling of the knee and designing of custom made knee implant using mimics software [32]. Here, CT images were used as an input data for modeling of the knee which produced an accurate model of the distal femur and proximal tibia. Segmentation using reliable profile line function was used in order to achieve an exact 2D surface which was further stacked together to convert it into 3D geometry. The results showed that implant designed using the reverse engineering procedure in mimics was found exactly negative to the patients distal femoral and proximal tibial bone. Curvature of the condyle part was exactly matched to the parent bone; providing the patient almost natural degree of motion in flexion and extension case. Thus it was concluded that segmentation supported by thresholding and profile line function ensured that only desired part involved in the knee model. Also, converting the geometry into surface mesh and importing it in STL format can be used to validate the knee model along finite element analysis. The polyline function can be smartly used to create the surface and can be imported in order to convert the surface into customized implant.

In their discussion of Knee Joint Segmentation, Y. Sun et al provided an overview of the current segmentation techniques for knee joint from medical imaging, such as computerized tomography (CT) and MR (Magnetic resonance) [33]. A review was made on the current segmentation methods which included: (1) thresholding approaches, (2) region growing approaches, (3)

classifiers,(4) clustering approaches, (5) Markov random field (MRF) models, (6) artificial neural networks, (7) deformable models, and (8) atlas-guided approaches. Typical methods of pixel-based segmentation consisted of thresholding, region growing and region merging etc. The geometry-based segmentations included deformable models such as snake, active contours, and active appearance models. Also, segmentation methods for knee joint structures included: Bone segmentation, Cartilage segmentation, Ligament segmentation. The study thus described a framework of the knee joint segmentation system followed by the strategies that would provide an accurate and precise segmentation. How these methods can be used in segmenting specific structures of knee joint are presented and their benefits and weaknesses are discussed.

Selection of Image Data from Different Imaging Systems

Each medical imaging modality has a specific physical principle so as to provide characteristic in vivo image data for various tissue types within a body section. For the geometric modeling of patient-specific anatomy, it is essential to select a proper imaging modality. Whenever opting for the imaging modality, some of the features like contrast-to-noise ratio, signal-to-noise ratio and image artefact types must be considered seriously. CT images are best suited for bone modeling in case of orthopedic applications, since hard tissue has a high contrast as compared to soft tissue. On the contrary, MRI images are more suitable for modeling of soft tissue due to the greater tissue resolution, where it is easy to distinguish tendons from muscles and cartilage from bone. Reasonable segmentation cannot be conducted as in a CT image separation cannot be obtained clearly because of the small differences in signal intensity between these types of tissue (Table 1).

Table 1 Comparison between X-ray CT system and MRI system

COMPARISON BETWEEN X-RAY CT SYSTEM AND MRI SYSTEM		
X-Ray CT system	**MRI system**	
Principle of Imaging	Absorption of X-Ray	Magnetic resonance phenomenon
Radiation Exposure	Yes	No
Tissue resolution	Good (Physical	Excellent (Scientific

	Information)	Information)
Dynamic diagnostic information	Difficult	Easy
Influence of Bone, Air	Yes	No
Image Plane	Transverse Plane	Arbitrary Section Plane
Examination Noise	Comparatively quiet	Large
Examination time	Short (5-10 min.)	Long (15-30 min.)
Preferred area	Lung, abdomen, bone,etc	Brain, Spinal Cord, Junction, etc.

The CT and MRI images can be differentiated on the basis of physical principle behind these medical imaging modalities. CT depends on X-ray radiation and the pixel values quantify tissue density, also known as attenuation coefficient or Hounsfield unit; hard tissues appear in the image with a high signal as they greatly attenuate high energy radiation.

However soft tissues, like muscle and fat, appear with lower signal intensity and less image contrast as they are more transparent to X-rays, hence discrimination of different types of contiguous soft tissue becomes difficult for CT. In relation to MRI, this method uses a powerful magnetic field in order to align the nuclear magnetization of the hydrogen atoms of the water molecules within the body. As compared to CT images, MRI images present a high soft tissue contrast because of a large variation in tissue-specific parameters that affect the MR signal thereby allowing the acquisition of images with greater contrast between different soft tissues. Furthermore, in an MRI image of the tissue-specific parameters, the effect on the contrast can be suppressed or enhanced by another set of operator-selectable parameters (such as repetition time, echo time and flip angle).

To generate a model of a specific anatomical structure it is necessary, first of all, to identify the tissues that compose the organ(s). Then, according to the desired image features, an appropriate medical imaging modality is chosen for data acquisition. For all cases here reported CT imaging is the proper selection [34].

The literature study tells us about the important factors affecting the movement of knee joints they are magnitude of ground reaction force, position of the knee relative to stress tensor and movement of the femur, tibia and patella. Although the biomechanical events related with each

part of the knee joint, the stress magnitude is the main factor that affects the activity of all parts which is required to be determined during different type of activities of knee. In the current study we have planned to geometrically model the knee joint as much real as we can with the help of computed tomography (CT) data followed by finite element analysis for finding the stress magnitude using ANSYS. Overall, the study presents a relation in the stress magnitude in different components of knee joint and will be helpful in providing a guideline for fabrication of prosthetic implant in the line of intimation with reduced number of experiments so that implants with better stress management and enhanced load bearing capacity can be designed.

CHAPTER 3

SOLID MODEL GENERATION OF KNEE JOINT

In the succeeding section a brief overview will be provided on how the computational model of knee joint were structured and what basis was taken into consideration. CT images were used for reconstruction of subject-specific geometry of articular lower limb surfaces.

Three-dimensional Finite Element model of the healthy human knee was recreated by CT-DICOM images utilizing image processing algorithms that incorporated the main structures of the knee joint bones. A general system of the FE bodies was evolved to create 3-D models from medical image data which is furnished in following layout (Figure 12).

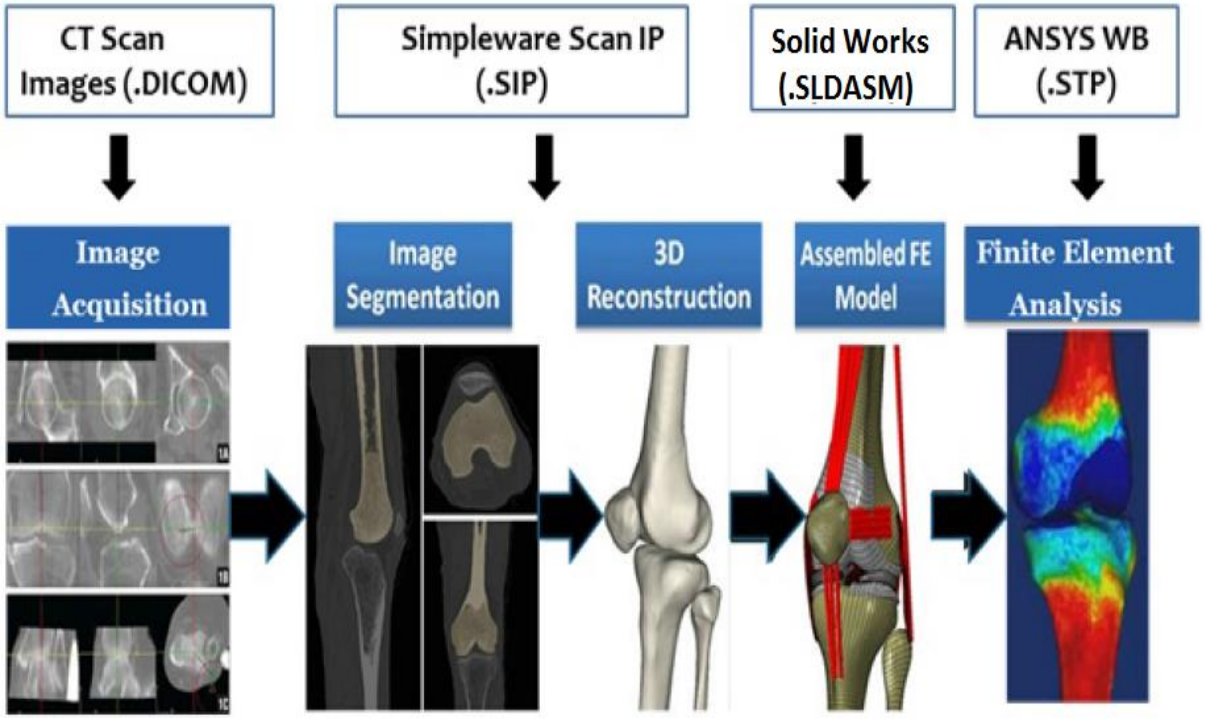

Figure 9 Representation of the software pipeline and its associated file

The steps followed to generate the 3D solid model of the knee joint can be set down as: - The first step involves Image Acquisition in which CT (Computed Tomography) images of lower extremity of a person with healthy bones are acquired in DICOM, Digital Imaging and Computation in Medicine, construct.

The second step was the segmentation of the obtained image data, where the image data is imported in Simpleware Scan IP 7.0 which is image processing software. The regions of interest were segmented by using threshold tool followed by split/merge tool and other filters like cavity fill, close filter and smoothening filter. This generates a 3D reconstructed model with only the components of interest i.e., completely segmented femur, tibia, fibula and patella bone in this case. The input data was provided in DICOM format while image processing and data storage was done in .SIP format. Further, NURBS solid model was initiated to generate the triangulated (i.e., STL) mesh which is easily supported by all available CAD packages

The third step was the generation and assembly of solid model of knee joint components. Here, 3D solid model of femur, tibia, fibula and patella bones are imported as IGES format in SOLIDWORKS (which is a Computer Aided Design package) and put together to create knee joint.

3.1 Image Acquisition

CT scan images of lower extremity of a person (age 30 years, female) with healthy femur, tibia, fibula and patella bones were obtained. The images acquired have vascular phase and were obtained from a 64 slice CT scanner, GE Medical System, apparatus power condition were at 120 KV/350mA. The images acquired were in DICOM (Digital Imaging and Communication in Medicine) format. The folder containing DICOM images were imported to the trial licensed copy of Scan IP 7.0 for further 3D Image visualization, solid model generation, analysis & meshing. The resolution of images was 512x512 with the slice thickness of 0.576172 pixel spacing in both X &Y directions.

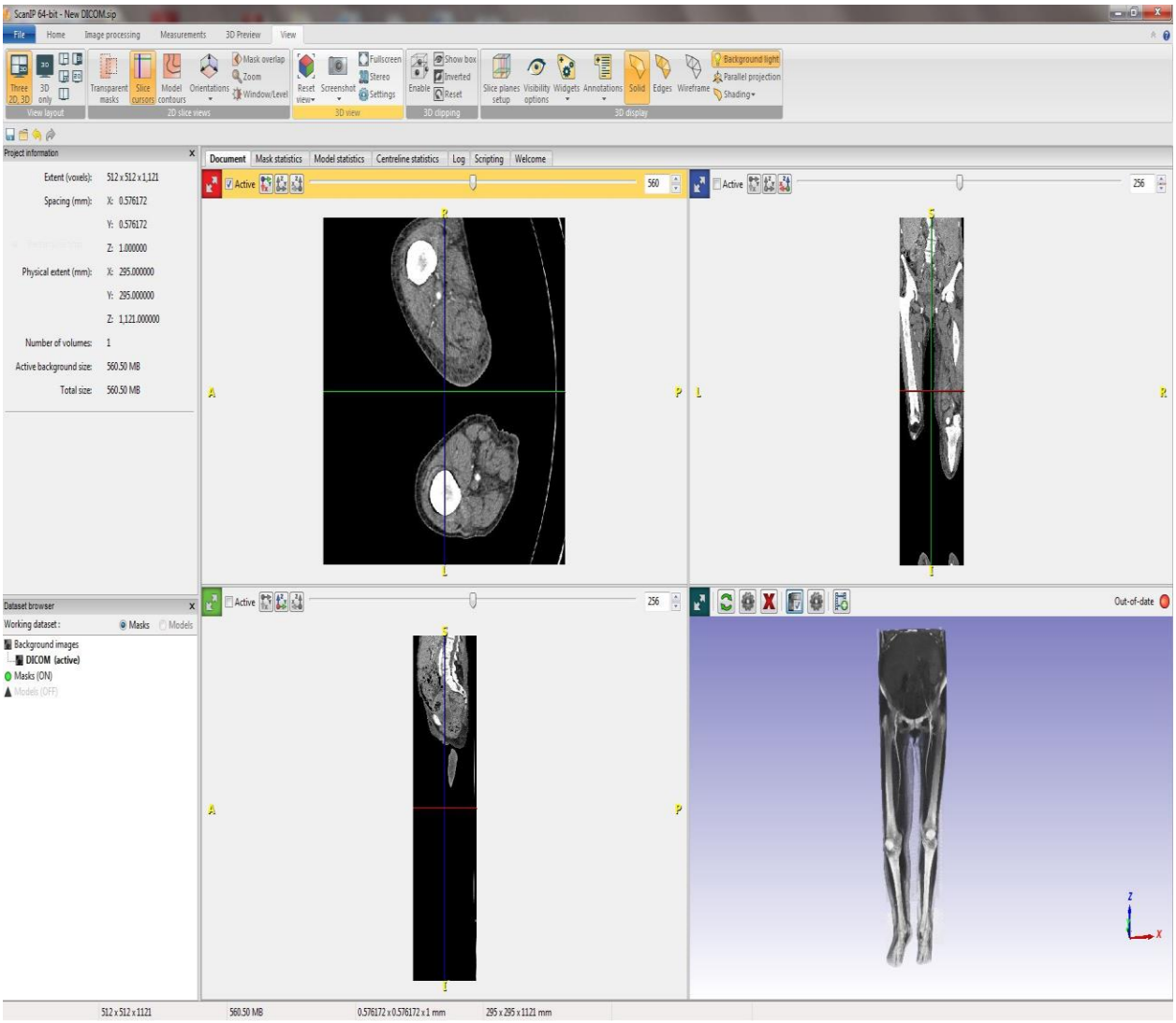

Figure 10 Visualization of the acquired CT image of complete lower extremity of patient.

3.2 Preparing the Acquired CT Data

In presence of image artifacts and signal noise it is necessary to better the resolution and quality of the CT images by proper acquisition parameters as slice thickness and spatial resolution. Also, various digital image processing techniques can be carried out in order to enhance the visual information encompassed in an image.

3.2.1 ***Computing the histogram*****: -** The loaded image data was then developed for visualization in axial, coronal and sagittal planes. After visualization of the images in the preview, a histogram (Grayscale range -2000 to 2000) was calculated [35] and set to a customized range of window: 300, level: 40 (Figure 13).

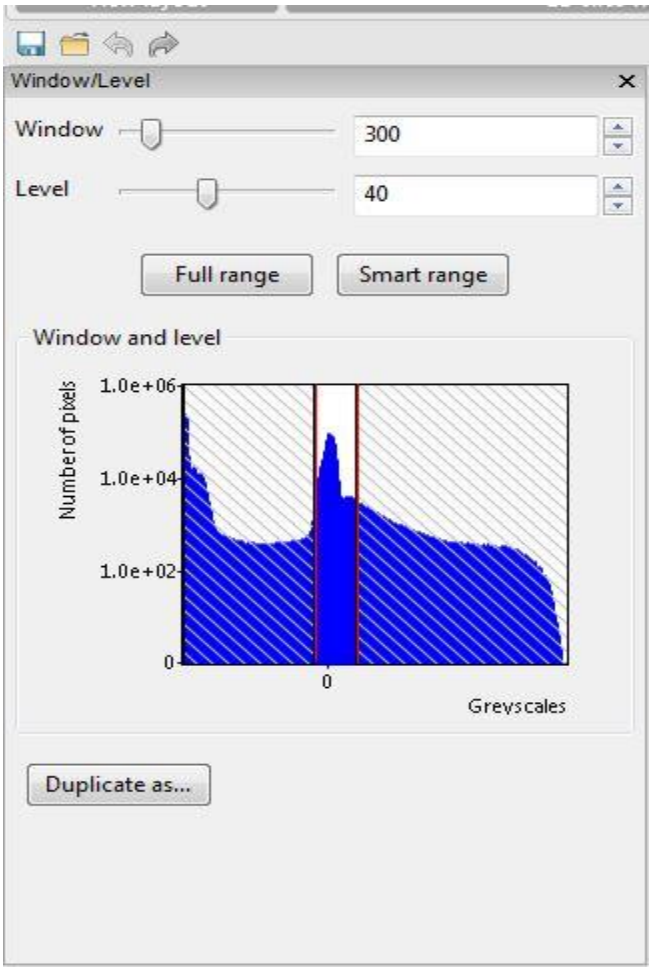

Figure 11 Histogram of the acquired DICOM images

3.2.2 ***Cropping:*** **-**Cropping is the simple operation of cutting off parts of the volume in order to only keep data of interest. Sometimes for memory usage purposes, it is recommended to crop your image in order to only keep the necessary objects within the limits of your volume. Cropping reduces the total no. of slices thereby reducing the computing time as well as reducing the tedious task of segmentation (Figure 12, 13).

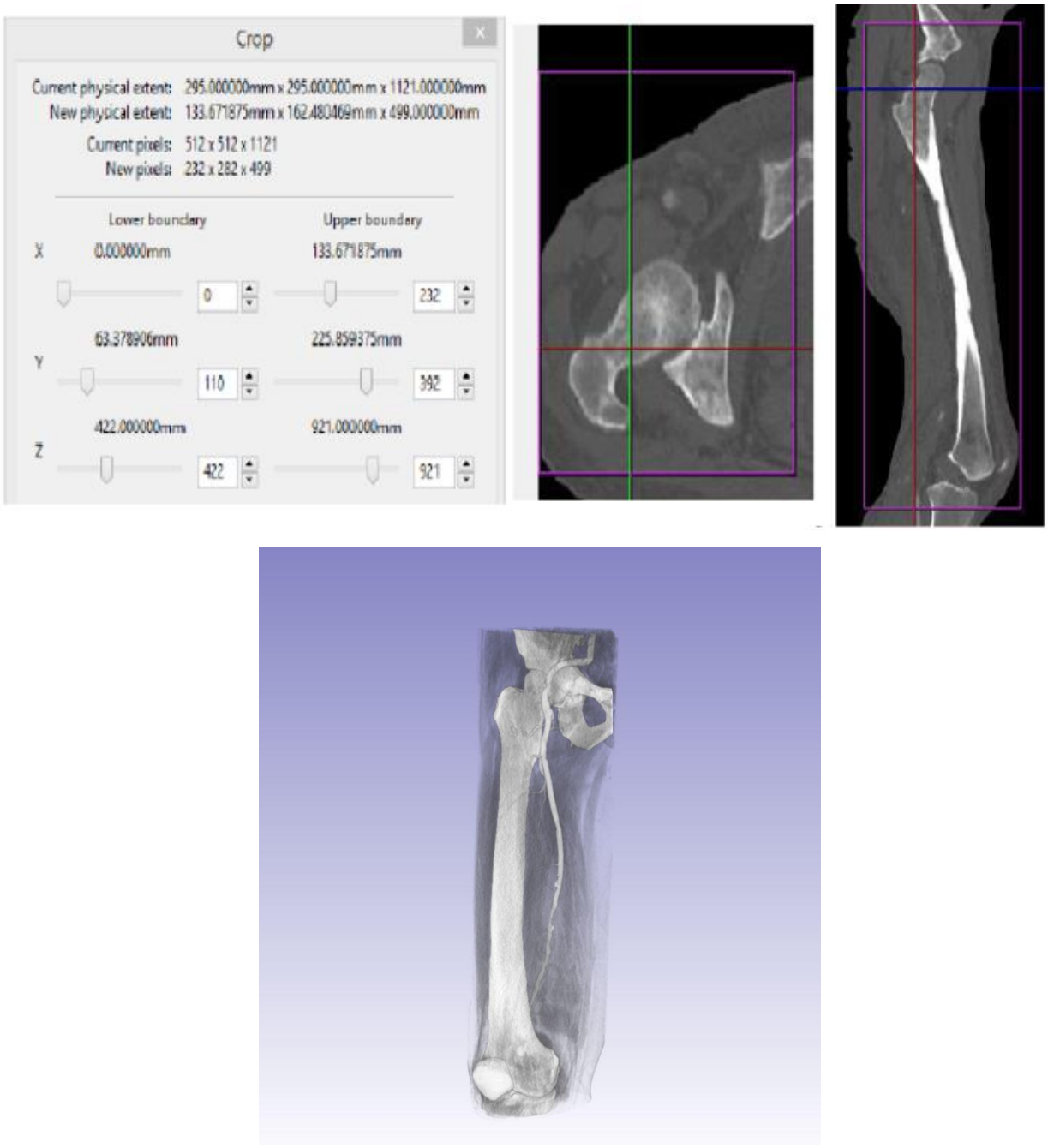

Figure 12 Snapshot of femur bone being cropped from CT scan image of complete lower extremity

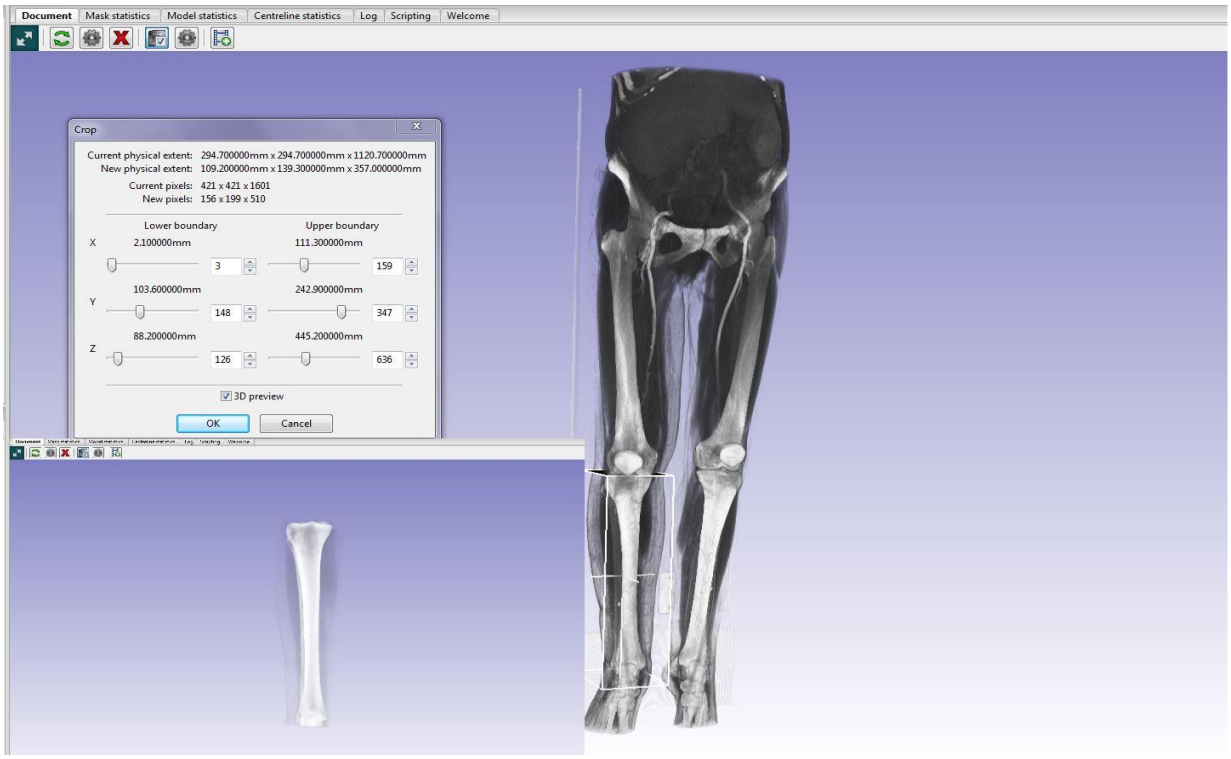

Figure 13 Snapshot of tibia bone being cropped from CT scan image of complete lower extremity

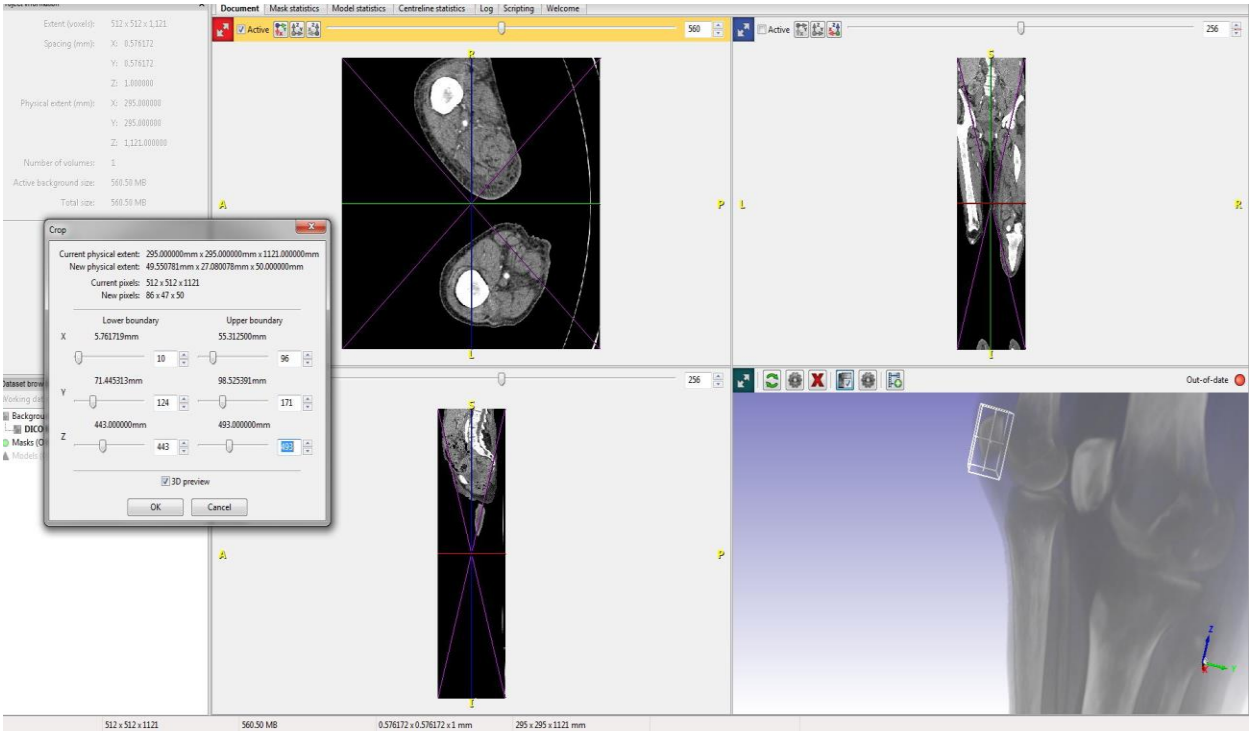

Figure 14 Snapshot of patella being cropped from CT scan image of complete lower extremity

3.3 Image Processing

Since, multiple image processing methods are available by which segmentation can be implemented [36]; it solely depends on the requirement as to what traits are to be obtained by the segmentation. Here, segmentation of the femur, tibia & patella bone from the full lower extremity of the CT scan of a person is done.

3.3.1 ***Segmentation*****:** The subsequent step in modeling is known as image segmentation, that is the segregation of images into non-overlapping areas. In this each area is the locus of an object. It performs an essential role in multiple medical imaging applications by making it simpler for the delimitation of anatomical constructs and other areas of interest. Generally, this delineation is established on a given image feature like texture or intensity, which is same within a area [37]. Segmentation plays a basic role for anatomical modeling as it forms the conversion between image data and 3-D mesh data. Although, when working with medical images, the segmentation is amongst the extremely difficult tasks to be done within the whole project. It should be considered that a medical image constitues of the data comparitive to the internal parts of the body of human beings, but also of unwanted signals. Objects and blurred ends are some of the features usual to any medical image. Multiple segmentation approaches exist and can be chosen corressponding to the input image. Considering that CT images are the foundation of 3 dimensional medical information for the generation of knee joint constituting the tibia, femur and patella. However, segmentation includes a chain of processes, including the ones mentioned above, ScanIP uses the terminology Segmentation for tools that usually use data from the background image to change and/or generate a mask. Segmentation tools can be entirely manual (**Paint**), or supported (**Threshold**, **Paint with threshold**, **Region growing, Flood fill**). Since none of the tools are entirely automated they will need some capability and training in order to provide acceptable results. The phases in the segmentation process are defined for femur below. Similar steps are followed for patella and tibia.

3.3.1.1 Threshold**: -** Threshold chooses a space of greyscale standard values and is used where segmentation can be attained on the basis of greyscale intensities. The threshold tool chooses all the voxels in the working background image which has a greyscale value in the designated range. Empowering the interactive Threshold will allow to see the impact

when sliding the upper and lower value sliders. The standardization instruments can be used to calculate the “right” values to use in the Threshold. Often, the assortment is carried out by simply making use of the interactive threshold and selecting an appropriate range by seeing through eye. Greyscale range of 158-1647 is selected. A mask of red colour is used . A Mask is a collecttion of voxels and it overlays the Background image. It is created to choose the areas of interest, then they are added to a Model.

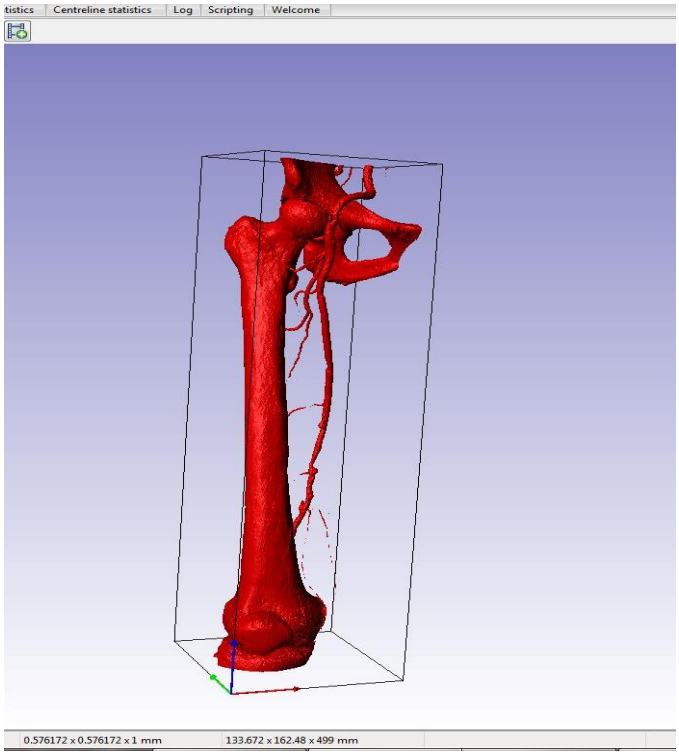

Figure 15 Femur after applying threshold tool

***3.3.1.2 Split/Merge Tool* : -** The Split/Merge tool is employed to help the end user in slicing masks that should not be connected but have been joined in the segmentation process, or to combine masks that should be connected but were not joined in the early segmentation.

- **Split**: Slice a mask into multiple masks or areas.
- **Merge**: Merge multiple masks or areas together.

Markers are employed to direct the **Split/Merge** tool to the objects that need to be sliced or combined. This is accomplished with the help of a correction mask. When we are executing a **Split** action, the correction mask must comprise of two/multiple distinctive markers for each object that is required to be sliced. When executing a **Merge** task, the

correction mask must be 1 continuous marker running across the edges of the objects that required to be merged.

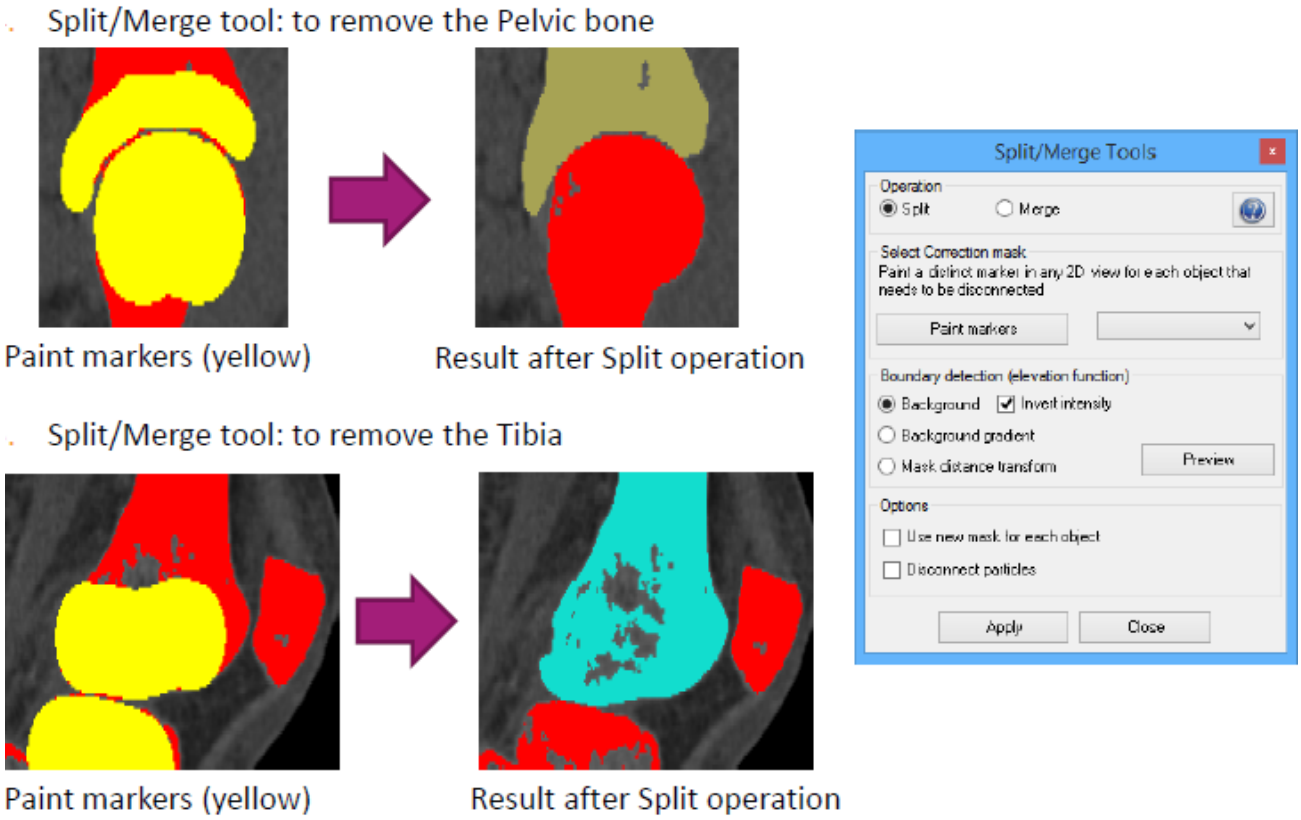

Figure 16 Using split/Merge tool in removal of pelvic and tibia bone from femur

The segmented femur after the use of split/Merge tool is shown in the following figure

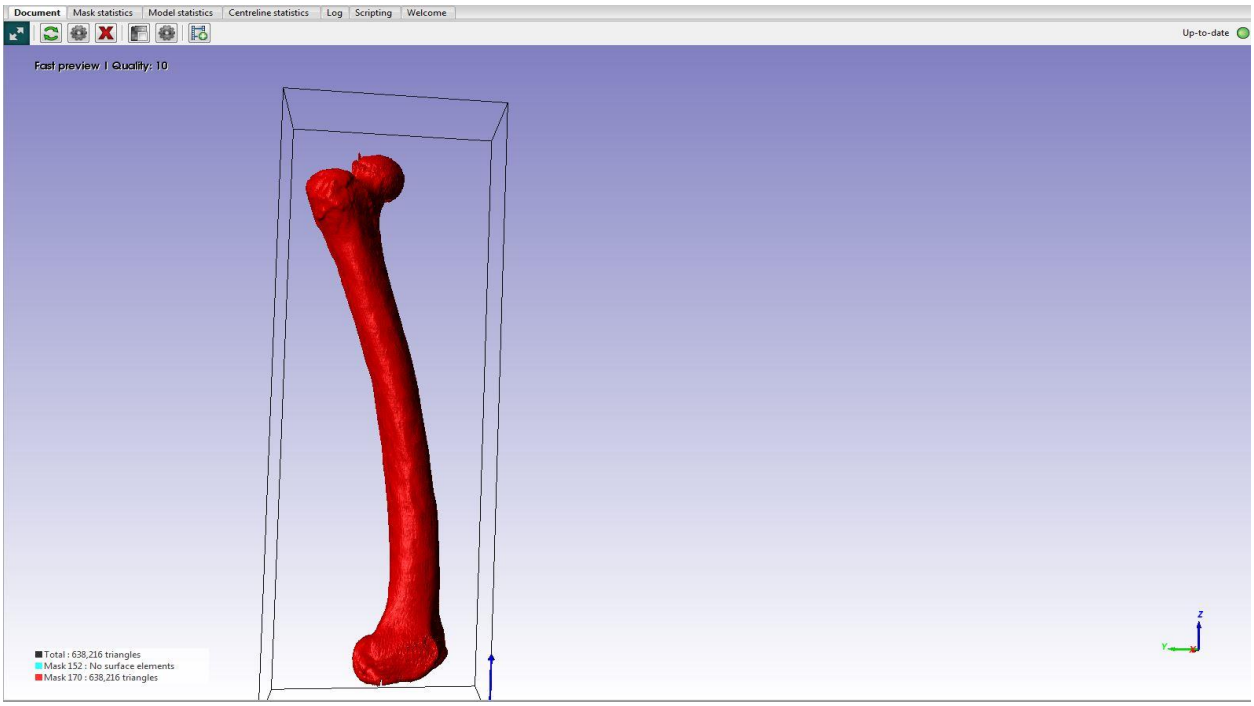

Figure 17 Segmented femur after using split/Merge tool

3.3.1.3 Smoothing Filter:- Following the completion of the whole segmentation procedure, a sample of the segmented bone is created. It is then assesed properly to find any holes/patches in the generated model geometry. Recursive Gaussian filter is used for the smoothing of each mask of the 3D model. It, typically, minimizes image noise and decreases detail levels (Figure 20) [39].

The visual impact of the blurring method is a smooth blur and it is also employed as a pre-processing phase in computer vision algorithm. This is done in order to improve image structures at diverse scales.It is, mathematically, similar to convolving the image using a Gaussian or normal distribution. Since, the Fourier transform of a Gaussian is also a Gaussian, it has the same impact as that of a low pass filtered image.

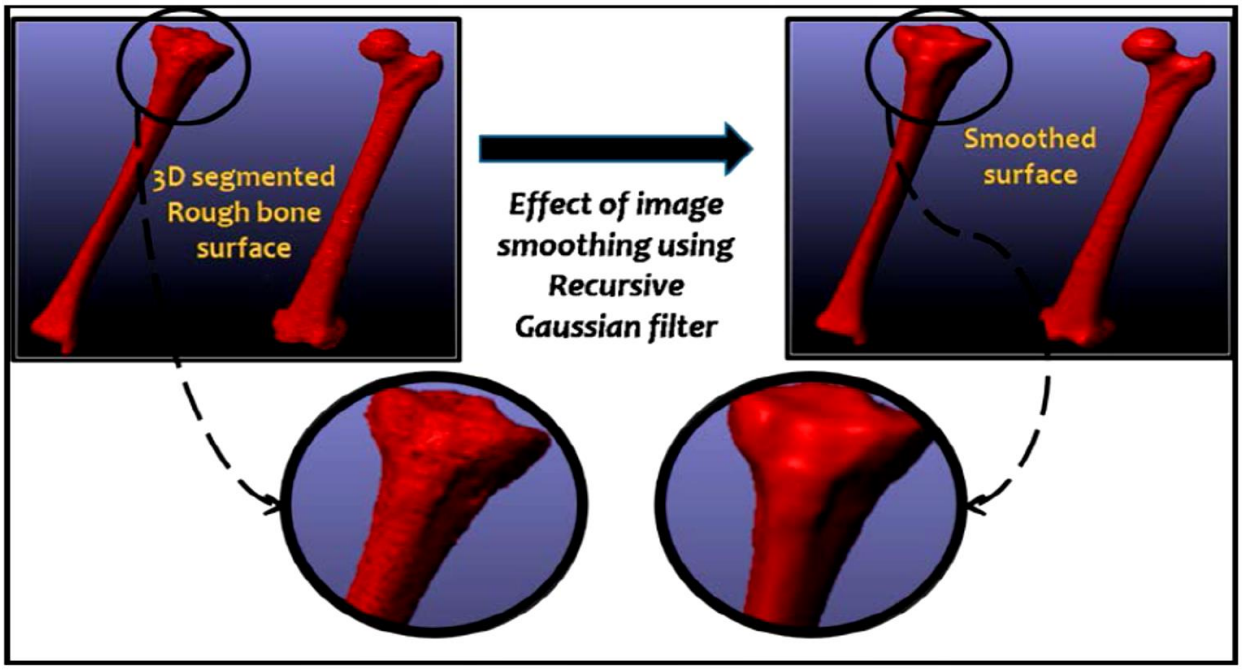

Figure 18 Application of image smoothing (Recursive Gaussian) filter and its result

Since. there are holes over the mask of the segmented femur, these holes are required to be closed prior to smoothing process. There is a requirement to apply **Close** first prior to employing smoothing task that is a morphological filter. It was applied with a value of 3 (cubic values) on the present mask. Now the cavities are also filled using **Cavity Fill** filter on the active mask. After all these operations the image is smoothed by applying Recursive Gaussian filter on active mask with Gaussian sigma value as 2.5. A Gaussian sigma value between 1 to 3 is preffered for smoothing. Figure showing the final segmented tibia and patella after smoothing operation is shown below

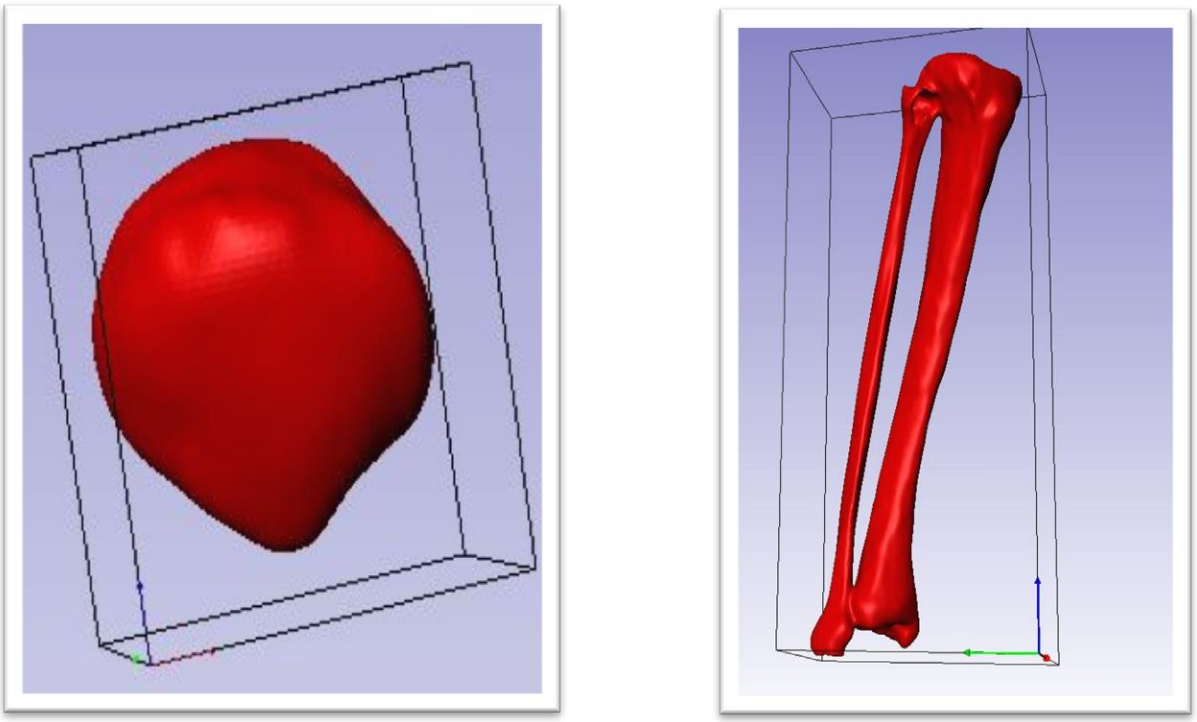

.

Figure 19 Final segmented patella and tibia

The femur, tibia and patella mask are now ready to be added to a NURBS model.

3.4 Solid Model Generation of Bone Morphology

The modelled area of interest is later converted to IGES format with transformed polygen surface to logical non-uniform b-splines surface (NURBS). These are logically described surfaces on the basis of control points [40]. The computation and description of NURBS is an important usefulness in comparison to distinct tessellated areas. In one way, this permits an improved functioning of CAD model; on the other way, the logical surfaces can be scattered like an automated hexahedral or tetrahedral meshing task can be helped. The faceted areas are transformed into NURBS appropriately; the bone can be transmitted to a pre-processor with the help of the IGES boundary. On condition that the surfaces develop a waterproof body, the solid can later be meshed with tetrahedral finite elements. It was further imported into CAD packages (SOLIDWORKS) for assembling and regeneration of knee joint.

3.4.1 Generating and exporting a NURBS surface from a model

Following steps were involved in this module:-

3.4.1.1 Preparing the Segmentation

Prior to creating the NURBS surface, it was important to ensure that the segmented masks were properly prepared. The surface features of the geometry mainly decide the success of fitting a NURBS surface as well as the final quality of the patches. Since, the patches will attempt to surface all existing features, so, a mask with small spurious features or rough patches will reduce the quality of NURBS patches. It was important to remove any unwanted features from the segmentation as the NURBS surface fitting is feature preserving. This reduces the need to generate flawed NURBS patches and therefore reduces the possibility of NURBS algorithm failing to create a valid surface.

The morphological CLOSE filter removes any patches thereby reducing the amount of data loss in the mask whereas the Recursive Gaussian smoothing filter is used to make the mask as smooth as possible. The model for NURBS fitting is then created by successfully optimizing the segmentation and ensuring that the mask is ready and sufficiently smooth (Figure 19).

3.4.1.2 Creating a Model for NURBS fitting: - The NURBS model generation includes two major steps: Firstly, a triangulated surface was created using the parameters in the General and surface settings tab in Model Configuration tool. The triangulated surface was then used as the input to fit a NURBS surface using the parameters in NURBS fitting tab (Figure 20).

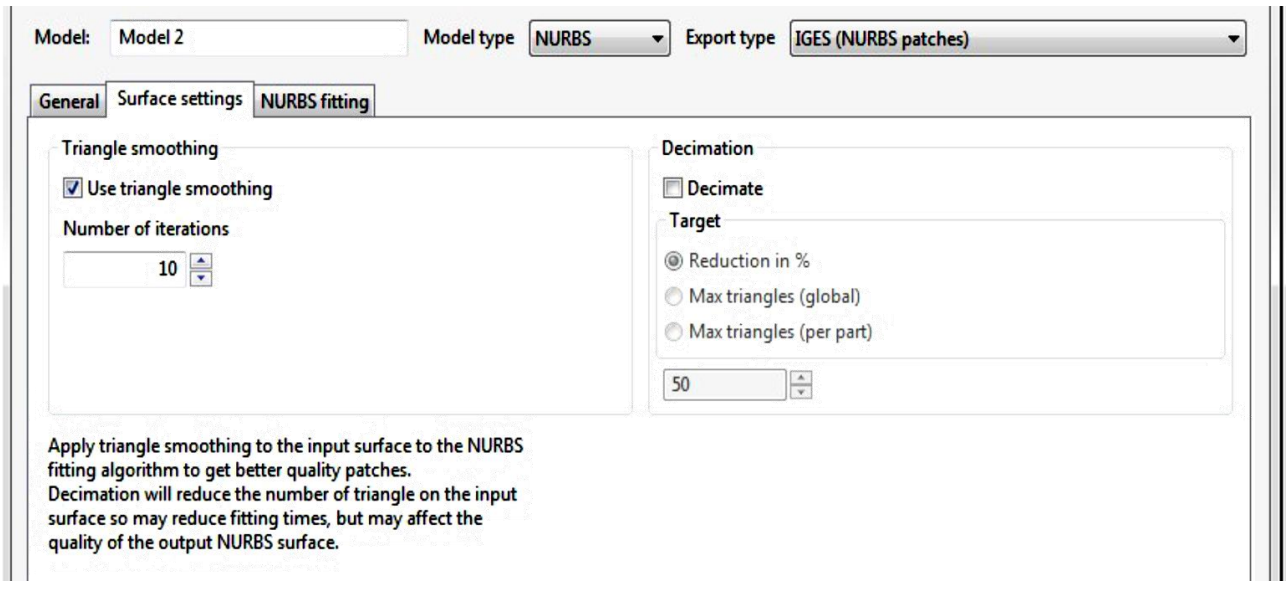

Figure 20 Window showing surface fitting parameters in Model Configuration tool.

The NURBS surface was created, successfully configured and then inspected to focus on locating small surface artefacts that if left would cause NURBS algorithm to fail or produce invalid NURBS patches. The level of triangle smoothing was increased and the surface model was regenerated if such artefacts were present (Figure 20).

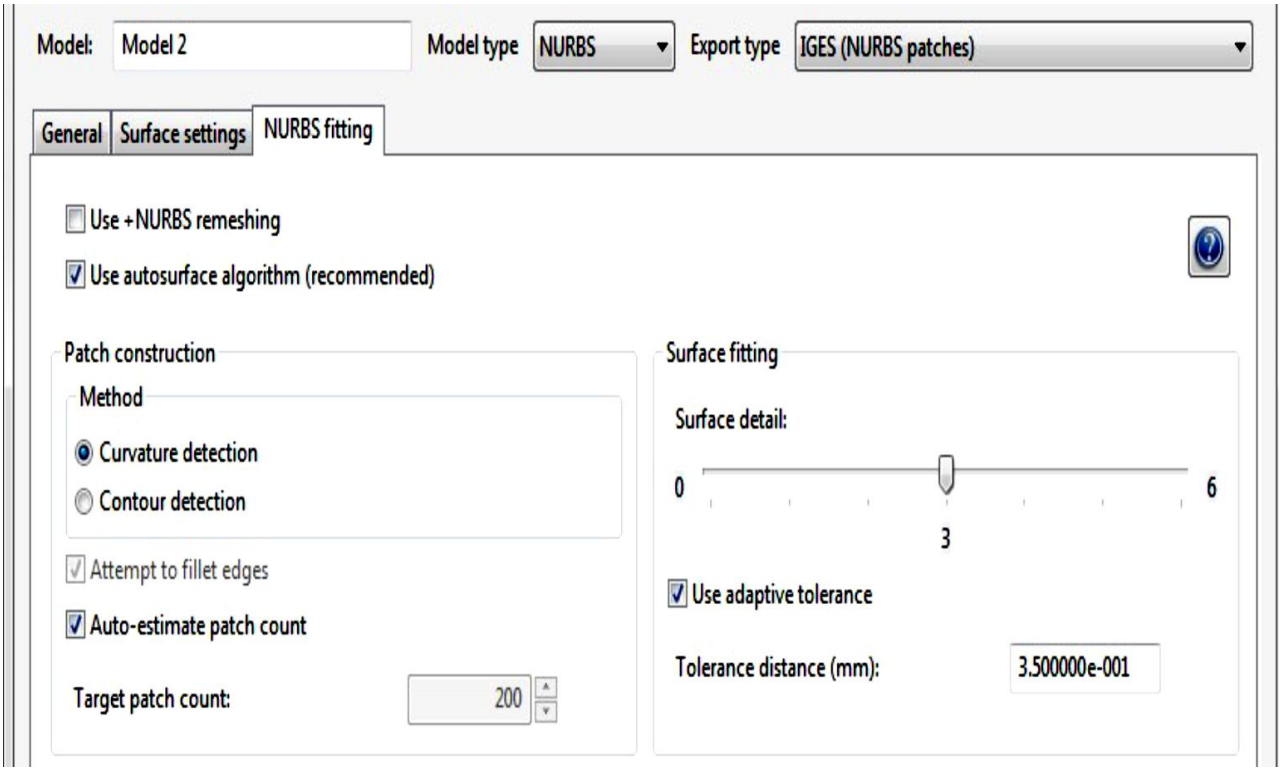

Figure 21 Window showing NURBS fitting parameters in Model Configuration tool.

3.4.2 Preview the Surface Model and Launch the NURBS Algorithm

NURBS model preview was generated to create the triangulated (i.e. STL) mesh (Figure 21). The generated surface model was inspected to check the smoothing settings and segmentation quality. It was then required to launch the NURBS algorithm. Finally, solid (NURBS) model/ FE model of femur, tibia and patella was generated and exported in IGES format (Figure 22).

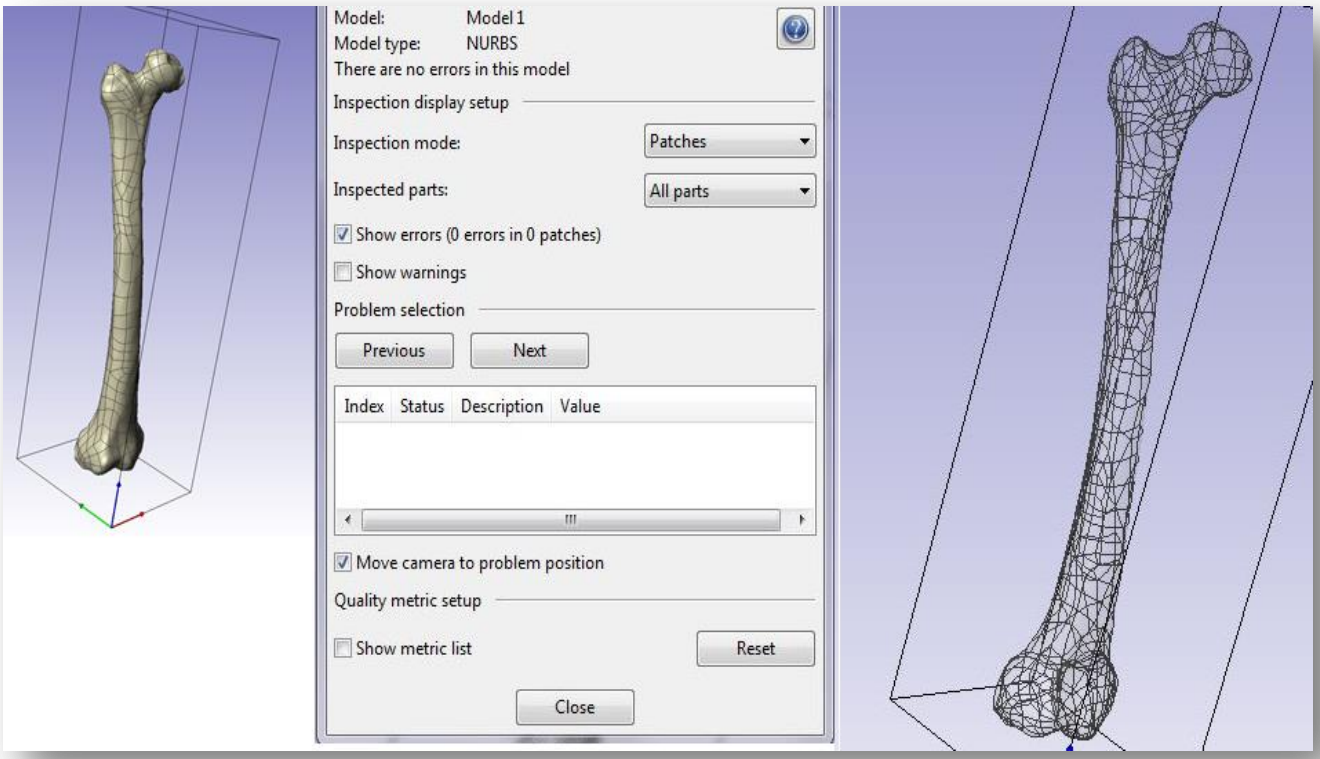

Figure 22 A sneak of the NURBS surface model and quality inspection parameters for femur

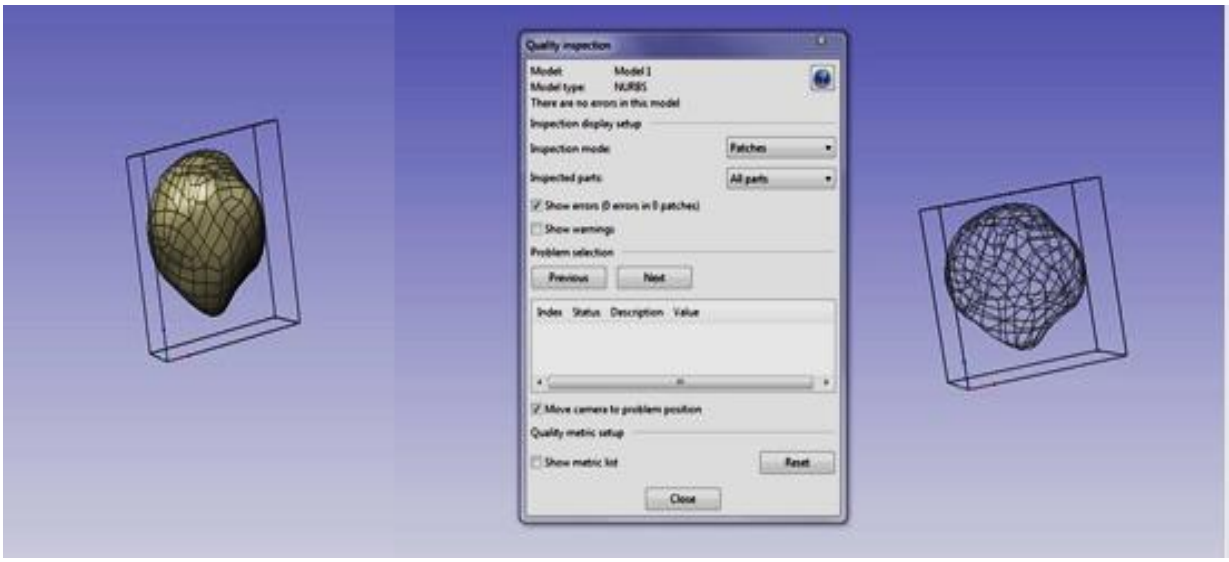

Figure 23 A sneak of the NURBS surface model and quality inspection parameters for patella

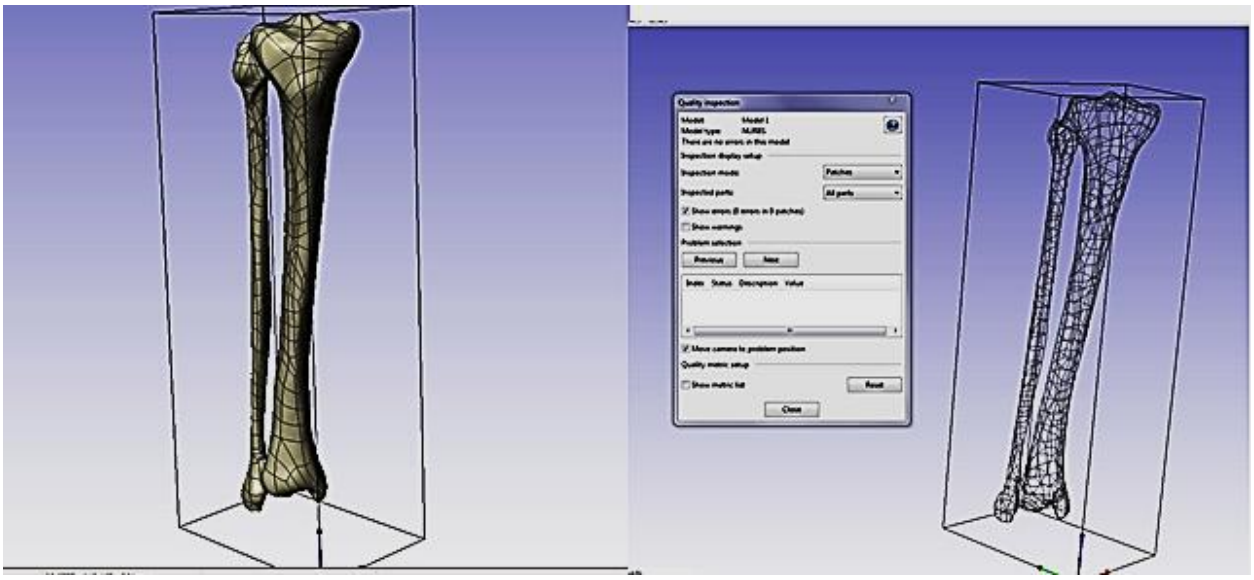

Figure 24 A sneak of the NURBS surface model and quality inspection parameters for tibia

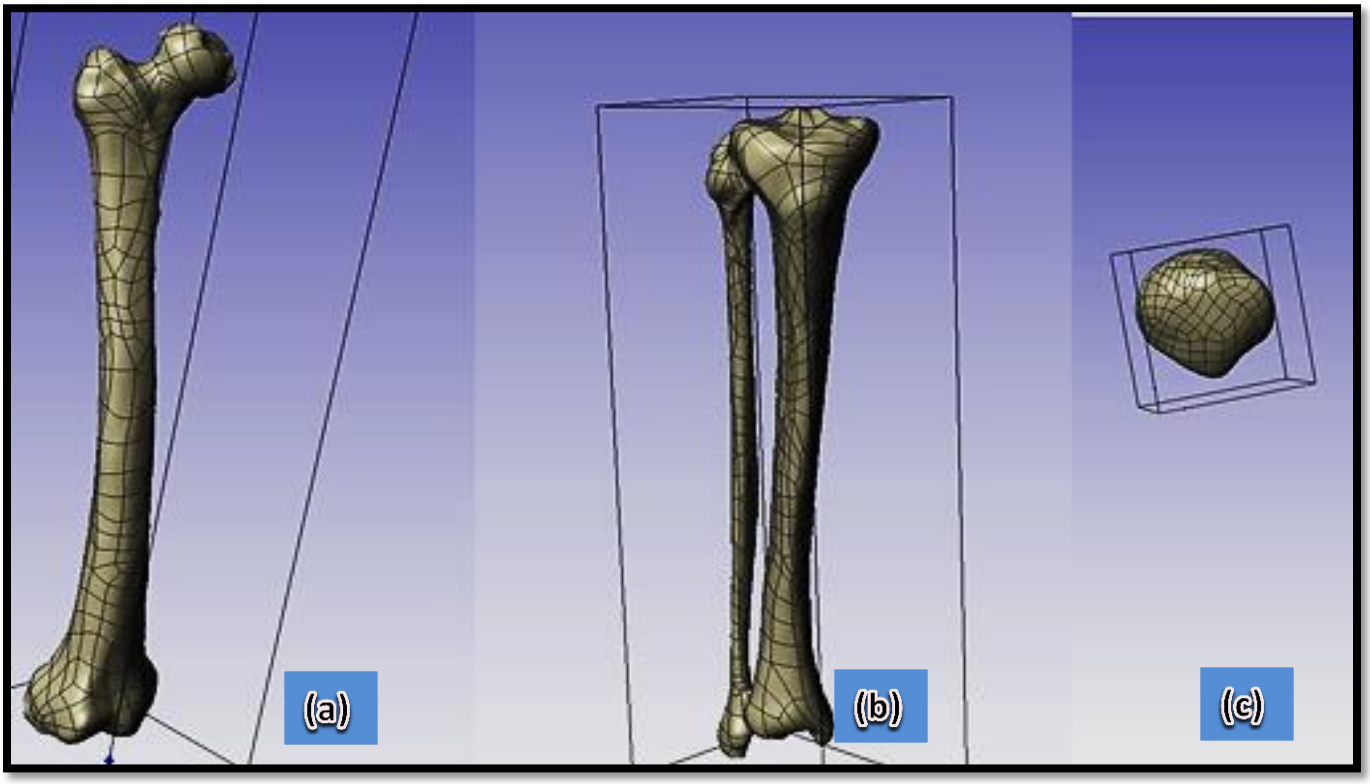

Figure 25 Solid (NURBS) model of (a) Tibia (b) Femur (C) Patella with NURBS mesh in IGES format

CHAPTER 4

SIMULATION METHODOLOGY

This chapter deals with an overview of Finite Element Analysis (FEA) usage and simulation setup. The criteria to reconstruct anatomical structure of knee and alignment analysis are also discussed here. Reconstruction of knee joint and stress analysis of different cases was done using SOLIDWORKS (CAD package) and all simulations were carried out in ANSYS WORKBENCH R15.0 (FE Simulation software).

4.1 Finite Element Analysis in Orthopedic Biomechanics

4.1.1 Purpose – The main purpose of Finite Element Analysis (FEA) in orthopedic biomechanics is to understand and predict the mechanical behavior of bones, develop design of implants with improvement, and eliminate/minimize the cost and time required in vivo and in vitro experimentation (Fig.). Finite Element modeling is also used for bone remodeling and healing phenomena of conventional and biomimetic devices, such as hip replacements [41] [42] [43]. Of late, computational modeling along with bone biology, biochemistry, and thermodynamics is being used to create new therapeutic strategies related to bone loss and other bone related diseases [44] [45] [46].

4.1.2 Principles – The advancement of FE models in orthopedic biomechanics begins with the data acquisition with the help of medical imaging techniques, such as magnetic resonance imaging (MRI) and computed tomography (CT) scans [47]. These scans must be of adequate resolution to allow for correct and accurate duplication of the geometries of interest.

The data is then converted into accurate 3-dimensional geometries of the bone tissue using the medical imaging software. The software must have a minimal or zero error known in the relative positioning of the image segments that constitute these 3 – dimensional regeneration. Computer aided design (CAD) software can be used for creating the geometry of prostheses to be implanted into bones or joints. In the FE model verification of the exact placement of the implant

into the bone tissue should be done using the X-Rays. This will help to replicate laboratory experiments or clinical scenarios accurately.

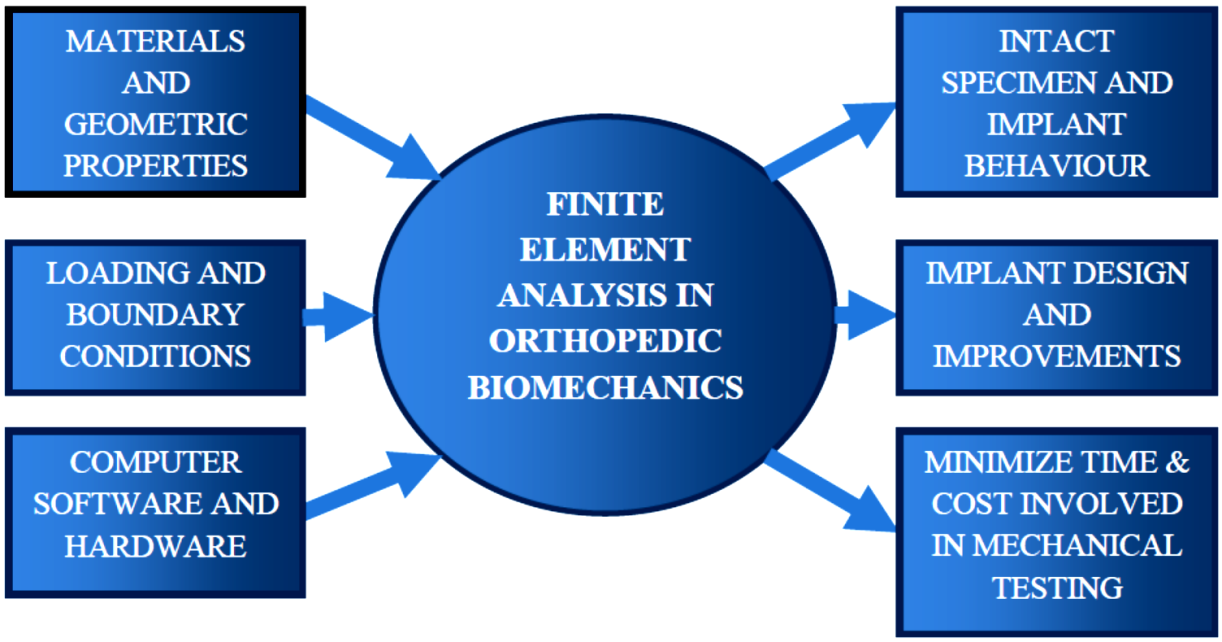

Figure 26 Overview of FEA showing required inputs and the outcomes.

The assembled geometry will then be ready to be exported into a software simulation package for further analysis. The bones and implants are then assigned the material properties and physiological load conditions that are reflective of real-world conditions are then applied. At this stage, finite element analysis (FEA) should be performed to obtain a variety of outcome measures, such as strain, stress, stiffness and/or strength. The accuracy of the FEA outcomes will depend on the assumptions made to create the FE model. It is important to understand the extent up to which such assumptions may impact the analysis of the results, given the fact that it is very challenging to generate and analyze a model without any assumptions.

Usually assumptions may involve input data, such as geometric and material characteristics, boundary conditions and loading, further analysis, and the understanding and explanation of results. Each of the assumptions has a set of limitations associated with it which will affect the computed end results.

4.1.3 Outcome Measures

Bone quality or stiffness, stress, strain, and strength are a few outcome parameters significant to engineers and clinicians.

4.1.4 Software and Hardware Required

To complete FEA of any structure three types of software are required. First, a computer aided design (CAD) package is required to create the solid model of the bone or implant (in this project SOLIDWORKS was used). Second, a finite element (FE) program package is required for analysis such as ANSYS. Third, to create a 3D model of complex geometries where density measurement is essential, such as bone tissues, medical imaging software (Mimics, Materialize Group, Leuven, Belgium, Scan IP) processes CT images and converts them into 3D models. The bone can then be put together to imitate the test setup and can be exported for analysis to ANSYS Workbench (ANSYS Inc. Canonsburg, PA, USA). It is advised to use a computer known for speedy numerical data processing since FE models often require significant computational time, in order to minimize central processing unit (CPU) time and storage expenses (in this project DELL Precision T7600 Workstation with 12GB RAM and high end computing XENON Processor was used).

4.1.5 Data Assessment

Data analysis in FEA can be either statistical or structural in nature. Statistical analysis enables the prediction of the uncertainty in the modeling variables on the biomechanical behavior of the bone implant system. For example, stochastic approaches such as the Monte Carlo method can be used to evaluate the probability of bone fracture under static loading conditions. Structural analysis allows the quantification of normal and shear stresses, strains, and strain energy densities, as well as investigating different failure modes of the bone and/or implant under physiological load conditions.

4.2 Universal Setup for Finite Element Bodies Used In Study

In order to perform FE simulation 3D solid model of femur and tibia which was generated by above steps discussed in chapter 3, was imported in SOLIDWORKS to reconstruct knee joint in assembly mode (Figure 27).

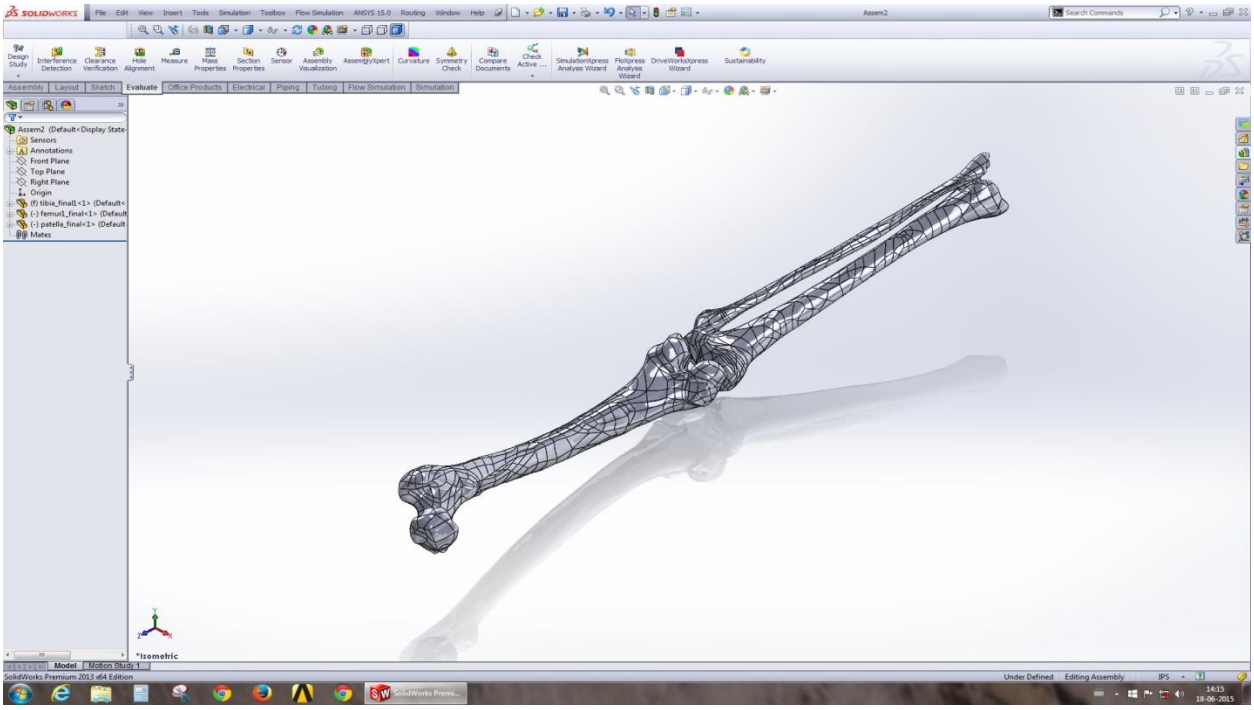

Figure 27 Reconstruction of the femorotibial joint from developed solid model of femur and tibia.

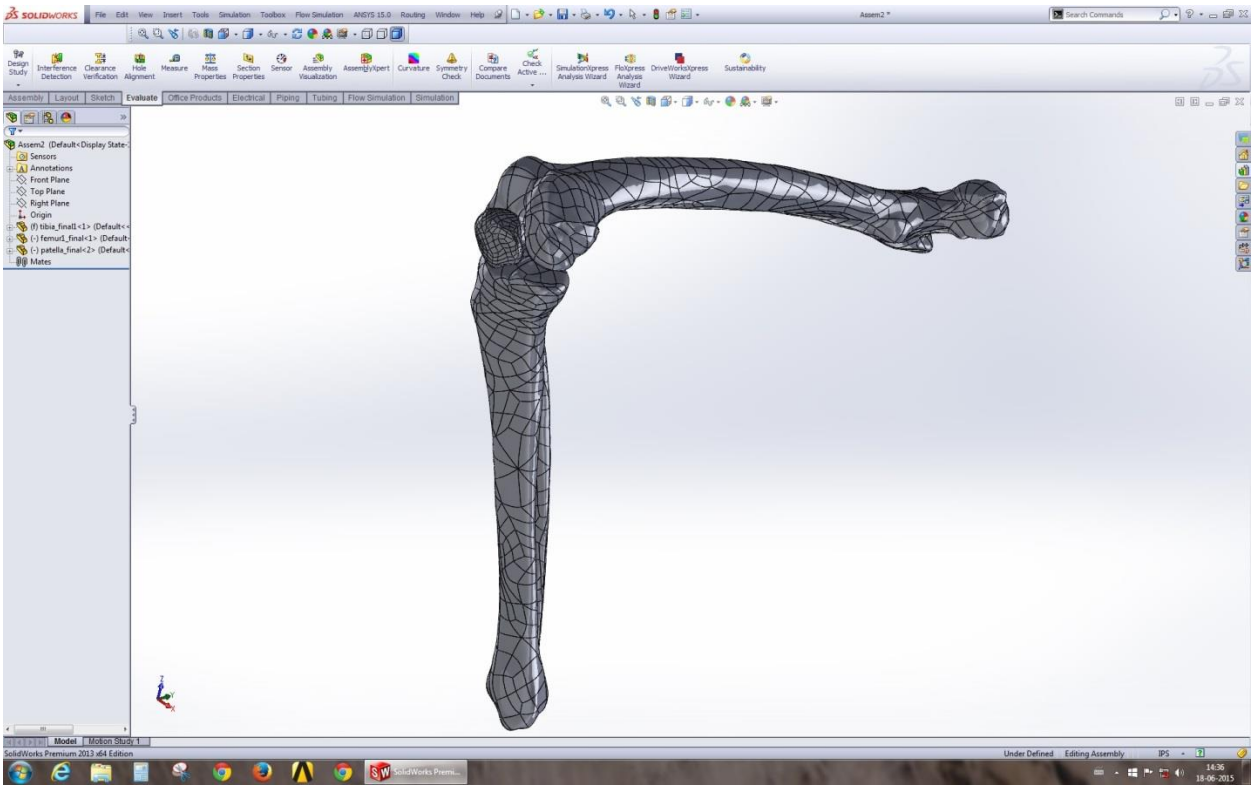

Figure 28 Reconstruction of the knee joint at 90^0 flexion

Constructed knee joint was imported in Ansys Work bench R15.0 as an associated IGES file where simulation was done (Figure 29).

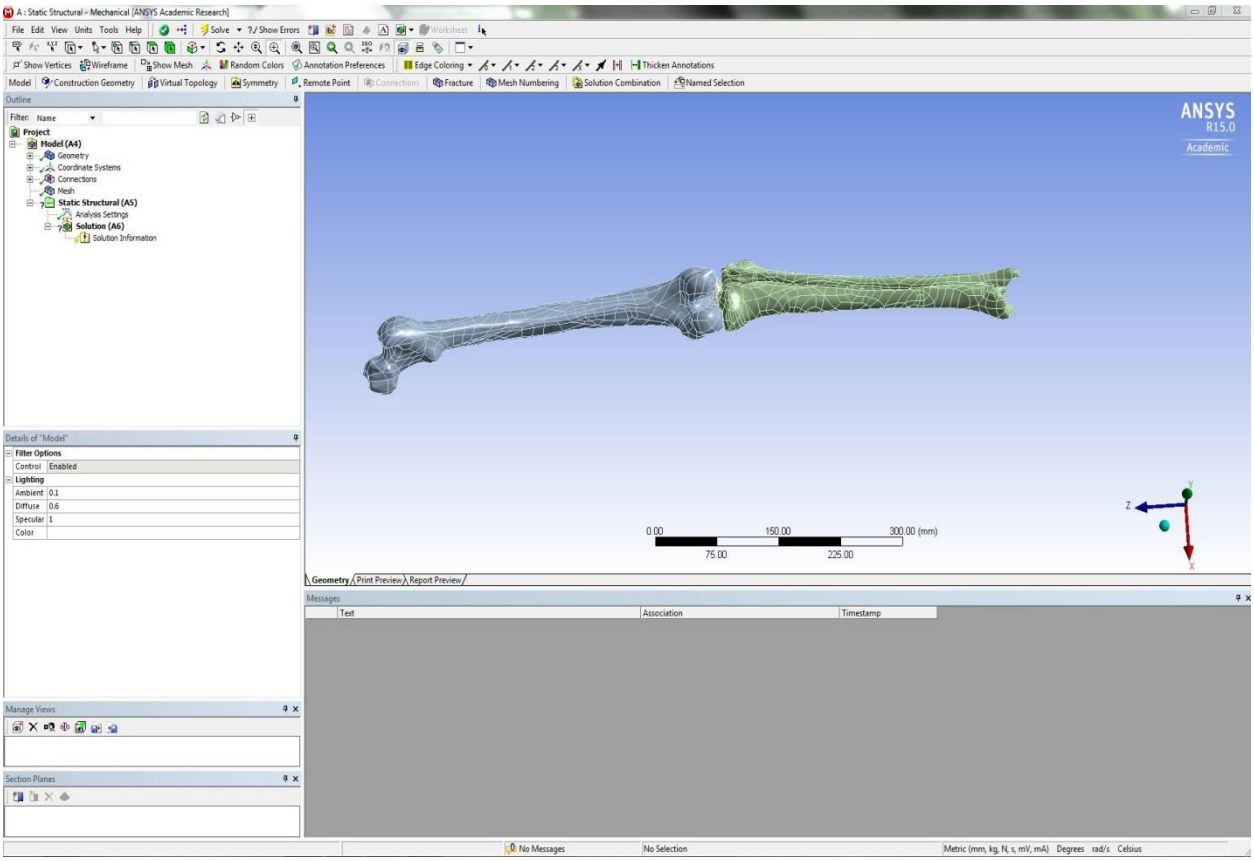

Figure 29 Illustration of the femorotibial joint exported to ANSYS Workbench for Analysis.

4.3 Material Assignment

Bone behavior was approximated by a homogeneous isotropic linear elastic material. The average mechanical properties of each type of bone tissue are shown in Table 1 which was extracted from CES selector (Cambridge Engineering Selector, an engineering materials selection tool). The lower boundary of the bone properties was selected for these simulations because most of the patient which undergoes TKA is elderly having problem of bone degradation or osteoporosis which weakens the mechanical property of bone.

Table 2 Table of the material properties of bone used for the simulations (From CES selector).

Structural Properties of bone	Value
Young Modulus	1.7e10 Pa
Poisson's Ratio	0.31
Density	1.8e3 kg/m^3
Thermal Expansion	1e-5 /°C
Tensile Yield Strength (elastic limit)	1.2e8 Pa
Compressive Yield Strength	1.14 e8 Pa
Bulk Modulus	* 1.8e10 Pa
Values marked * are estimates	

4.4 Loading and Boundary Conditions

4.4.1 Force analysis of knee joint

By using static analysis the forces and moments acting on a joint during no motion and incase of dynamic activities like walking ,lifting or running are determined. A Free body diagram technique is used which limita the analysis in one plane. Three principle coplanar forces acting on the free body are considered and designated in the free body diagram. The two cases are considered here. In first case the whole weight of the body is considered to be acting over a single knee joint just as in standing position. In second case force analysis is done for dynamic activities like walking or lifting. The various forces acting on knee joint in various motion are as follows:--

Fx - Friction Force

Fy - Ground Reaction Force

Fz – Ground To Foot Force

X – Perpendicular distance along Fy

Y - Perpendicular distance along Fx

P - Pattela Tendon Force

J - Joint Reaction Force

W - Ground Reaction Force

a- perpendicular distance alongW

b –perpendicular distance along P

Case1:When the total body weight is acting over a single knee joint in straight position:

In the first case, to calculate the two coplanar forces (Fx and Fz) acting on the foot the measurement is done from the line of action of force from the ground by considering the vertical force Fy as the body weight. On tibia there are three external forces acting which consists of the three ground-to foot forces (Fx, Fy, and Fz). Fx is the frictional force which is acting at the foot in the line of advance or progression; vertical component is Fy and Fz is the ground-to-foot force acting side-to side.The turning moment in the saggital plane of the knee joint can be estimated from: Mz = Fy × X and Fx × Y (Fig. 30). The distances X and Y are measured from the knee joint and the coordinates for the center of the pressure of the foot. Knee moment Mx in the coronal plane is calculated from: Mx = Fy × Z and Fz × Y.

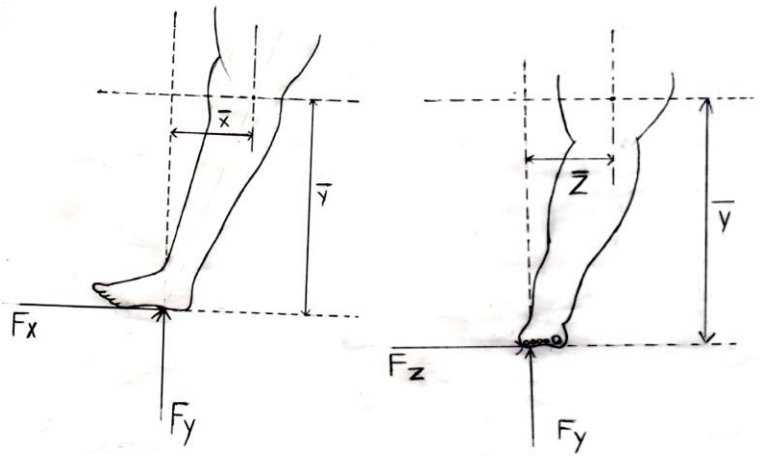

Figure 30 Representation of coplanar forces acting on knee joint during standing position.

Fx × y = Fy × x Fy × z = Fz × y

588.6 ×10 = Fz × 53 Fz = 111.05N

Fx × 53 = 588.6 × 15 Fx = 166.57N

The forces for different varying weight considered are calculated analytically for case-I and are shown in table 2

Table 3 Coplanar forces acting during standing position for different weights

WT(Kg)	Fy(N)	Fx(N)	Fz(N)
55	539.55	152.20	101.20
65	637.65	180.46	126.31
75	735.23	208.23	138.82

Case-II: During dynamic activities i.e walking or lifting, the leg is inclined and total weight of body acting on ankle.

For second case, an example explains the application of the free body technique for coplanar forces to the knee joint. The technique is used to calculated the minimum magnitude of the tibio-femoral joint reaction force of the weight bearing leg as the other leg is lifted while stair climbing. As per the literature studied there are two main forces acting on knee joint during walking and stair climbing position. They are patella tendon force (P) and joint reaction force (J) with the ground reaction force (W) as per the body weight. The vector diagram and the distance upto knee joint from the vertical force is measured practically to calculate the forces acting on the joint are. These are shown in figure(31) .

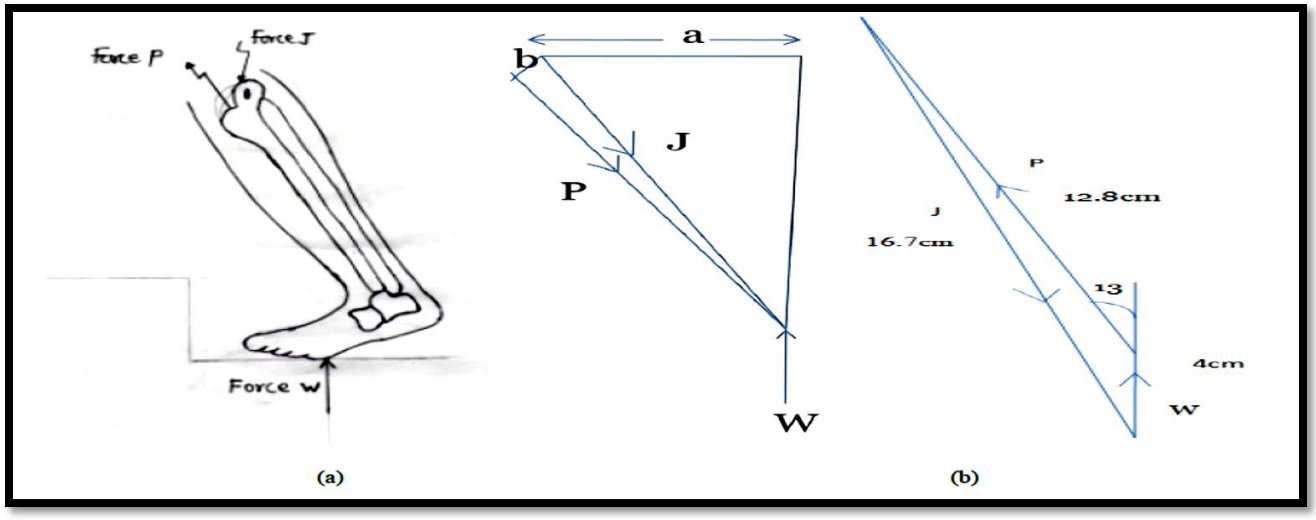

Figure 31:a)Free body diagram of knee joint for CaseII b)Vector diagram

ΣM=0

W×A - P×B = 0

W×A = P×B

P = 588.6×16.5/5.156= 1883.52

P = 12.8×147.15 = 1883.52N

J = 16.7×147.15 = 2457.405N

W = 588.6N

Similarly the forces for different body weights considered are also calculated analytically for case-II and are shown in table 3.

Table 3 Forces acting on knee joint during dynamic activities

WT(Kg)	Platellar tendon force(N)	Joint Reaction Force(N)
55(539.95N)	1726.26	2266.11
65(637.65N)	2040.48	2648.7
75(735.75N)	2354.4	3090.15

4.4.2 Boundary conditions

Varying weights are considered and the forces are calculated accordingly in table 2 and table 3. FE analysis of knee joint is carried out for different loading conditions . Analysis has been carried out for (i) vertical force (ii) 3-coplanar forces (iii) patella tendon force and joint reaction forces at 90^0 flexion. In all these cases the top part of the femur is fixed and it is assumed that whole body weight is supported by one leg. The other boundary conditions for these three analysis is explained below:-

I. Vertical force:- Vetical force is acting at the bottom surface of tibia
II. 3-coplanar force:- The Frictional force(Fx) is acting at front surface, the ground force(Fy) is applied at the bottom surface and the ground to foot force(Fz) is applied to side surface of tibia.
III. 90^0 Flexion:- The ground force is applied at the bottom surface, the tibiofemoral joint reaction force is applied at joint and the patellar tendon force is applied on the patella.

4.5 Virtual restrictions in reconstructed femorotibial joint

Linear approximation was done i.e. joint was provided 6^o of freedom with restrictions on large deflection, similar to ligaments of the knee which restricts motion within the joint but not fully. These restrictions are regenerated virtually in ANSYS by implementing weak springs in between the articulating surfaces.

4.6 Meshing

The details regarding the mesh generated are obtained from the report generated from Ansys15.0. The mesh report is shown below:-

Object Name	*Mesh*
State	Solved
Defaults	
Physics Preference	Mechanical
Relevance	0
Sizing	
Use Advanced Size Function	Off
Relevance Center	Fine
Element Size	Default
Initial Size Seed	Active Assembly
Smoothing	Medium

Transition	Fast
Span Angle Center	Fine
Minimum Edge Length	0.610750 mm
Inflation	
Use Automatic Inflation	None
Inflation Option	Smooth Transition
Transition Ratio	0.272
Maximum Layers	5
Growth Rate	1.2
Inflation Algorithm	Pre
View Advanced Options	No
Patch Conforming Options	
Triangle Surface Mesher	Program Controlled
Patch Independent Options	
Topology Checking	Yes
Advanced	
Number of CPUs for Parallel Part Meshing	Program Controlled
Shape Checking	Standard Mechanical
Element Midside Nodes	Program Controlled
Straight Sided Elements	No
Number of Retries	Default (4)
Extra Retries For Assembly	Yes
Rigid Body Behavior	Dimensionally Reduced
Mesh Morphing	Disabled
Defeaturing	
Pinch Tolerance	Please Define
Generate Pinch on Refresh	No
Automatic Mesh Based Defeaturing	On
Defeaturing Tolerance	Default
Statistics	
Nodes	116459
Elements	67899
Mesh Metric	None

CHAPTER 5

RESULTS AND DISCUSSION

A 3D model of the knee joint was obtained from the CT image of the female subject and various measurements made using ScanIP tools. Measurements such as length of femur and tibia were done using ScanIP tools. At the end of simulation, 3D solid model of Knee joint in SOLIDWORKS was analyzed for static loading using the finite element package ANSYS 15.0. Mechanical parameters investigated in this study are Equivalent von-Mises stress, total deformation, maximum principal elastic strain and maximum principal stress. On the value scale, the higher values are indicated by red color and the lower values are indicated by blue color. The values increase from blue to red. The accuracy of FE model with reference to the real physiological conditions around the model determines the result. Analysis is carried out for three different cases of loading and boundary condition. The result obtained is shown in tabulated format.

5.1 FE Analysis of Knee Joint for Vertical Force

The FE analysis of the knee joint for force acting in the vertical direction in Ansys 15.0 requires the surface at the top of femur to be taken as fixed and the vertical force is applied at the bottom surface of tibia. The Equivalent von-Mises stress, maximum principal stress, Maximum principal elastic strain and total deformation for 540N force are shown in figure 34. The results are calculated for varying weight.

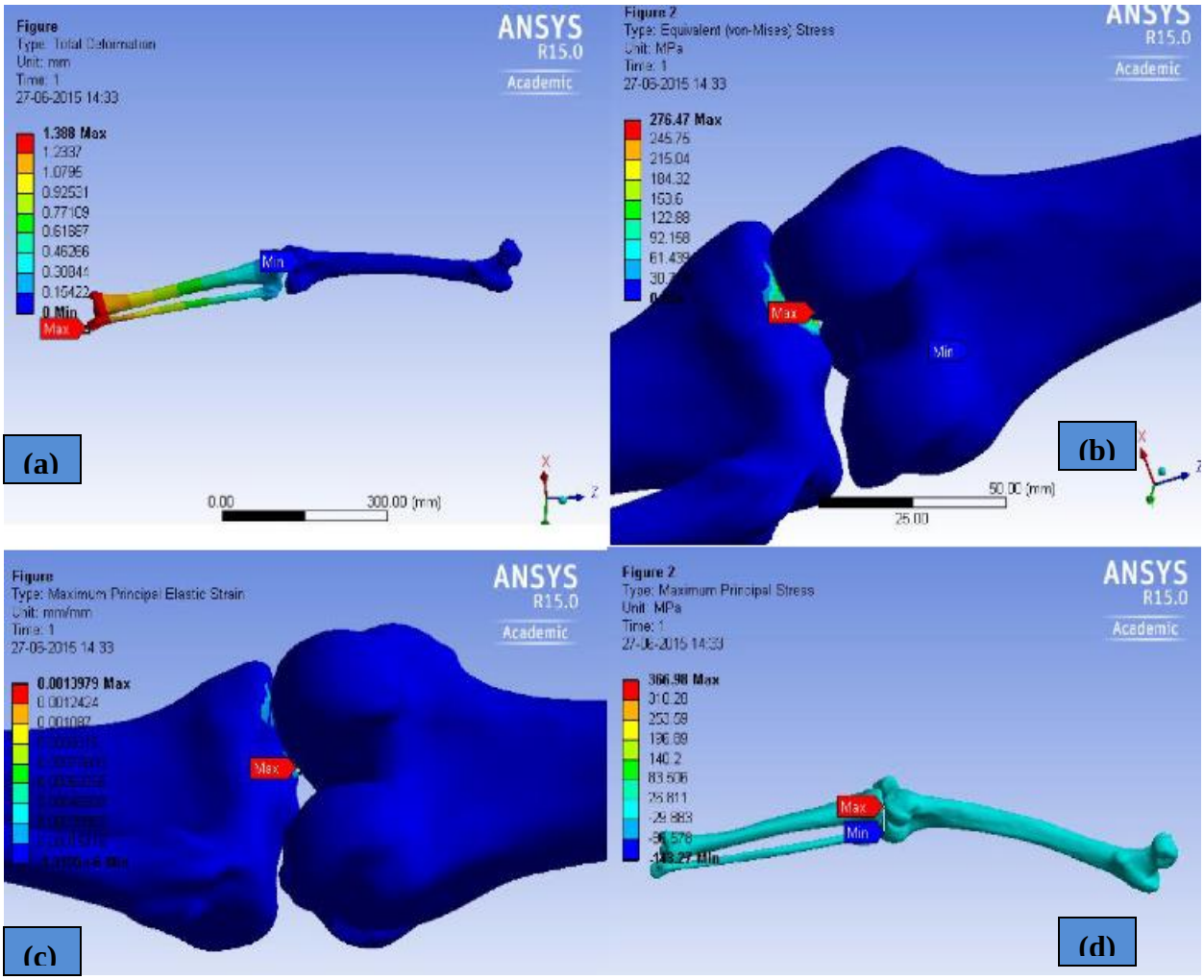

Figure 32 Total deformation (a), Equivalent von-Mises stress(b), maximum principal elastic strain (c)and maximum principal stress(d) for 540N

5.2. FE Analysis of Knee Joint for Three Coplanar Forces (Fx, Fy, Fz)

The FE analysis of the knee joint for three coplanar forces (Fx, Fy, Fz) in Ansys15.0 requires the top surface of femur to be taken as fixed and from table 2, the ground force (Fy) is applied at the bottom surface, the frictional force (Fx) is applied at front surface and the ground to foot force (Fz) is applied to side surface of tibia as depicted in figure 5(ii). The Equivalent von-Mises stress is calculated.

5.3. FE Analysis of Knee Joint for Patellar Tendon and Joint Reaction Force

For the FE analysis of knee joint for patellar tendon force in ansys15.0, the top surface of femur as taken as fixed and the ground force is applied at the bottom surface, the joint reaction force is applied at joint and the patellar force is applied on the patella along the condoler surface of femur. The Equivalent von-Mises stress is obtained .

Table 5 Maximum Von Mises stress obtained

Weights (Kg)	**Equivalent Von Mises Stress (MPa)**	
	Vertical force	**3 Coplanar forces**
55	4.45	2.32
65	5.93	3.09
75	10.9	3.88

The FE analysis has been performed in Ansys software and Von-Misses stresses for various conditions explained above have been found and are shown in table 5. From the result depicted in the table it can be inferred that the von-misses stresses increases continuously during steady environment for weight varying from 55 to 75 kg. Von-Misses stresses vary from 1.5 to 7.4 MPa and it increases more while walking at the range of angle from 10 degree to 90 degree. However, from the finite element analysis it has been observed that the stresses are changed exceedingly for dynamic conditions by taking into account the joint reaction force and the patellar tendon

force for different weight at 90 degree. By the study of process of TKA (total knee replacement), the implant is provided for the joint problems caused due to accidental injuries or diseases. The stresses have been found out, which are more than the stress experienced at normal conditions, but are safe up to a certain limit i.e. from 10 to 50 degree which increases tremendously after 50 degree but are safe at 90 degree. Table 4 shows the mechanical parameters examined at multiple load conditions.

The comparison of these results was done with various literature reported. The behavior of our results was similar to behavior of results reported in literature. Slight variations associated with these mechanical behaviors of femur were found due to high variation in material property and other physiological conditions.

Using this modeling approach, a next course of action, considering total knee replacement, implant designing, implant fitting and fracture treatment may be undertaken.

In orthopedic biomechanics, a number of approaches have been used to extract the geometry of interest from CT images such as MIMICS (Materialise Interactive Medical Image Control System), 3D Slicer, ScanIP and Amira. A drawback of these approaches is that their virtual memory usage is very high and as well as due to large size of DICOM file, when memory is not sufficient, the whole processing slows down. Therefore, high virtual memory computers are helpful to cut down this problem and also recommended to crop and resample the image so software will be able to process fast. The 3 dimensional FE models of the knee bones created from CT data is of interest these days due to its high importance in clinical procedures. The problem is one of creating a valid and accurate model which satisfactorily represents the real structural behavior of the human bone. By selecting appropriate Window width-level (W, L) and greyscale values would help in getting better segmentation which will result in a better model. Manual segmentation needs expertise or practice to get satisfactory results.

CHAPTER 6

CONCLUSIONS AND FUTURE WORK

In this work various literatures related to the problem statement have been studied and generation of full solid model & static structural analysis of knee was done. This whole process includes generation of 3D model from quantitative CT scan images, NURBS meshing, assigning material properties, applying loading & boundary conditions and analyzing the model.

After going through various literatures and from this study, it was found that the extraction of geometry of interest from CT image by using segmentation technique is the most laborious step. And if better segmentation and smoothing is done, meshing process will be easy and a good solid model will be generated.

Since the real anatomical structure of knee bones includes hard and soft tissue with bone marrow. Also, the physical conditions around the joint are much more complex as compared to this model, i.e., area around femoral head, neck and condylar region. Simulating all these issues, this work may be considered as a starting phase of computational analysis of biological structures by applying finite element method.

FUTURE SCOPE OF WORK

In the study of joint biomechanics one of the primary issues of using finite element method is that it is very time consuming to segment surface geometry from medical image data, which potentially limits the amount of subjects that could be analyzed in a given study. Developed models and results of analysis are helpful for the orthopedic surgeons to understand the mechanical behavior of the knee joint, in knee replacement surgeries and implant designing & fixation. Method for developing a real knee model and the developed model itself can also be used as a data base for the forthcoming students who are interested to do further work in this area of biomechanics.

It would be more challenging to develop a more real type knee model which also includes other hard and soft tissues. Developing a detailed 3D structure of femur is a problem that needs deeper consideration, given the issues observed. Also, the behavior of knee bones should be analyzed considering the physiological conditions around the bone joint.

Based on this study and work the experimental work on knee fabrication and hip implant can be performed. This will give a definite approach for fabrication of implant in less no of experiments in a cost effective manner.

REFERENCES

1. P.S. Walker and J.V. Hajek, “The load-bearing area in the knee joint,” *Journal of Biomechanics*, 1972, v. 5, n. 6, pp. 581–584.
2. J.R. Ralphs and M. Benjamin, “The joint capsule: structure, composition, ageing and disease,” *J. Anat*, 1994, v. 184(Pt 3), pp. 503-509.
3. www.orthoinfo.aaos.org
4. www.aboutstryker.com/pdfs/knee_replacement.pdf.
5. R. A. Siston, J. J. Patel, S. B. Goodman, S. L. Delp, and N. J. Giori, “The variability of femoral rotational alignment in total knee,” *J. Bone Joint Surg Am*, 2005, v. 87, n. 10, pp. 2276-2280.
6. R. A. Siston, J. J. Patel, S. B. Goodman, S. L. Delp and N. J. Giori, “The high variability of tibial rotational alignment in total knee arthroplasty,” *Clinical Orthopaedics and Related Research* 2006, v. 452, pp. 65-69.
7. T. D. V. Cooke, E. A. Sled, and R. A. Scudamore, “Frontal plane knee alignment: a call for standardized measurement,” *The Journal of Rheumatology*, 2007, v. 34, n. 9, pp. 1796-1801.
8. L. M. Lozano, M. Núñez, S. Sastre, and D. Popescu, “Total knee arthroplasty in the context of severe and morbid obesity in adults,” *The open obesity journal*, 2012, v. 4, pp. 1-10.
9. J. R. Moreland, “Mechanisms of failure of total knee arthroplasty*,” Clin Orthop*, 1988, v. 226, pp. 49-64.
10. SR Simon, H Alaranta, Orthopaedic Basic Science: Biology and Biomechanics of the Musculoskeletal System (ed 2), An KN, et al, Kinesiology, in Buckwalter JA, Einhorn TA, Simon SR (eds), American Academy of Orthopaedic Surgeons, 2000, pp. 730-827.
11. K.E. DeHaven, Articular Cartilage and Knee Joint Function: Basic Science and Arthroscopy, The role of the meniscus J.W. Ewing (Ed.), Raven, New York, 1990, pp. 103–115.
12. S.P. Arnoczky, C.A. McDevitt, Orthopaedic Basic Science: Biology and Biomechanics of the Musculoskeletal System (ed 2), The meniscus: Structure, function, repair, and

replacement J.A. Buckwalter, T.A. Einhorn, S.R. Simon (Eds.), American Academy of Orthopaedic Surgeons, 2000, pp. 531–545.

13. S.C. Shoemaker, K.L. Markolf, "The role of the meniscus in the anteriorposterior stability of the loaded anterior cruciate-deficient knee," *J. Bone Joint Surg Am*, 1986, v. 68, pp. 71–79.
14. F.H. Fu, C.D. Harner, D.L. Johnson et al, "Biomechanics of knee ligaments: Basic concepts and clinical application," *J. Bone Joint Surg Am*, 1993, v. 75 pp. 1716–1727.
15. F.G. Girgis, J.L. Marshall, A.R. Monajern," The cruciate ligaments of the knee joint: anatomical, functional, and experimental analysis," *Clin Orthopaedics*, 1975, v. 106, pp. 216–231.
16. Simon H Palmer, Mervyn J Cross, Total Knee Arthroplasty, Ed. M Mike Malek, Talavera, John W Uribe, eMedicine for WebMD, July 13, 2004,
17. www.arthritisresearchuk.org
18. C. Townley, L. Hill, "Total knee replacement," *Am J Nurs*, 1974, v. 74, pp. 1612-1617.
19. Jawahir A Pachore, Shrinand V Vaidya, Chandrasekhar J Thakkar, Haresh Kumar P Bhalodia, Hemant M Wakankar, "ISHKS joint registry: A preliminary report," *Indian Journal of Orthopaedics*, 2013, v. 47, n. 5.
20. Ali Sina Shahi, Hamid Reza Seyyed Hosseinzadeh, Gholam Hossein Kazemian, Aidin Masoudi, Mehrnoush Hassas Yeganeh, Usama Hassan, Samih Tarabichi and Hamid Reza Seyyed Hossein Zadeh Ardebili, Arthroplasty – Update, Special Considerations in Asian Knee Arthroplasty, Chapter 3, Plamen Kinov (Ed.), InTech, 2013.
21. C.S. Houston, L.E. Swischuk, "Occasional notes, Varus and valgus: no wonder they are confused," *J. Med*, 1980, v. 302, pp. 471–472.
22. K. Tetsworth, D. Paley, "Malalignment and degenerative arthropathy," *Orthop Clin North Am* 1994, v. 25, pp. 367–77.
23. Atul F. Kamath, Craig Israelite, John Horneff, Paul A. Lotke, "What is Varus or Valgus Knee Alignment? A Call for a Uniform Radiographic Classification," *Clin Orthop Relat Res*, 2010, v. 468, pp. 1702–1704.
24. S. Matsuda, L.A. Whiteside, S.E. White, "The effect of varus tilt on contact stress in total knee arthroplasty," *Orthopedics*, 1999, v. 22, n. 3, pp. 303–307.

25. G.M. Brouwer, A.W. Van Tol, A.P. Bergink, J.N. Belo, R.M. Bernsen, M. Reijman, et al, "Association between valgus and varus alignment and the development and progression of radiographic osteoarthritis of the knee," *Arthritis Rheum*, 2007, v. 1204, n. 11.
26. J. P. Jr. Barrett, E. Rashkoff, E.C. Sirna, A. Wilson, "Correlation of Roentgenographic Patterns and Clinical Manifestations of Symptomatic Idiopathic Osteoarthritis of the Knee," *Clin Orthop*, 1990, v. 253, pp. 179–183.
27. D. Cooke, A. Scudamore, J. Li, U. Wyss, T. Bryant, P. Costigan, "Axial Lower-Limb Alignment: Comparison of Knee Geometry in Normal Volunteers and Osteoarthritis Patients," *Osteoarthr Cartil*, 1997, v. 5, pp. 39–47.
28. MAQUEST PGJ, Biomechanics of the Knee, Springer-Verlag, New York, 1984.
29. Bart Van Gheluwe, Kevin A. Kirby, Friso Hagman, "Effects of Simulated Genu Valgum and Genu Varum on Ground Reaction Forces and Subtalar Joint Function During Gait*," Journal of the American Podiatric Medical Association,* 2005, v. 95, n. 6.
30. Eric Thorhauer, Motoko Miyawaki, Ken Illingworth, J. Andrew Holmes and William Anderst, "Accuracy of bone and cartilage models obtained from CT and MRI," Annual Meeting of the American Soc., 2010, pp. 775.
31. Jeff Caldera, Amir M. Tahmasebib and Abdol-Reza Mansouria, "A Variational Approach to Bone Segmentation in CT Images," Medical Imaging 2011: Image Processing, Benoit M. Dawant, David R. Haynor (Ed.), SPIE, 2011, v. 7962, pp. 15.
32. Ravikant Kamal and D. Ashok Kumar, "Three-Dimensional (3D) Modeling of the Knee and Designing of Custom made Knee Implant Using Mimics Software," *International Journal of Current Engineering and Technology*, 2013, v. 3, n. 2.
33. Y. Sun, E. C. Teo and Q. H. Zhang, "Discussions of Knee Joint Segmentation," International Conference on Biomedical and Pharmaceutical Engineering, ICBPE, IEEE, Singapore, 2006.
34. N. S. Ribeiro, P. C. Fernandes, D.S. Lopes, J.O. Folgado, and P. R. Fernandes, "3-D Solid and Finite Element Modeling of Biomechanical Structures, A software pipeline," *7th EUROMECH Solid Mechanics Conference, J. Ambrosio et.al. (eds.), Lisbon, Portugal*, 2009.
35. N. Ramesh, J. H. Yoo, and I. K. Sethi, "Thresholding based on histogram approximation," *IEEE Proc Vision Image Signal Proc*, 1995, v. 142, pp. 271-9.

36. N. Sharma, and L.M. Aggarwal, “Automated medical image segmentation techniques,” *Journal of Medical Physics*, 2009, v. 35, n. 1, pp. 3-14.
37. D. L. Pham, C. Xu and J. L. Prince, “Current methods in medical image segmentation,” *Annu Rev Biomed Eng*., 2000, v. 2, pp. 315-37.
38. J. Fan, D. K. Y. Yau, A. K. Elmagarmid, and W. G. Aref, “Automatic Image Segmentation by Integrating Color-Edge Extraction and Seeded Region Growing,” *IEEE transactions on Image Processing*, 2001, v. 10, n. 10.
39. I. T. Young, and L. J. V. Vliet, “Recursive implementation of the Gaussian filter,” *Signal Processing*, 1995, v. 44, pp. 139–151.
40. B. Starlya, A. Laua, W. Suna, W. Laub, T. Bradbury, “Direct slicing of STEP based NURBS models for layered manufacturing,” *J. Computer Aided Design*, 2005, v. 37, pp. 387-397.
41. H. Bougherara, M.N. Bureau, and L. Yahia, “Bone remodeling in a new biomimetic polymer-composite hip stem,” *J Biomed Mat Res Part A*, v. 92, n. 1, pp. 164-174.
42. R. Huiskes, H. Weinans, H.J. Grootenboer, M. Dalstra, B. Fudala, T.J. Slooff, “Adaptive bone-remodeling theory applied to prosthetic-design analysis,” *J Biomech*, 1987, v. 20, n. 11-12, pp. 1135-1150.
43. C. Hernandez, G.S. Beaupré, and D.R. Carter, “A model of mechanobiologic and metabolic influences on bone adaptation,” *J Rehabil Res Dev*, 2000, v. 37, n. 2, pp. 235-244.
44. H. Bougherara, V. Klika, F. Maršík, I.A. Mařík, and L. Yahia, (2010d), “New predictive model for monitoring bone remodeling,” *J Biomed Mater Res A*, in press.
45. R. Huiskes, R. Ruimerman, G. Harry van Lenthe, and J.D. Janssen, “Effects of mechanical forces on maintenance and adaptation of form in trabecular bone,” *Nature*, 2000, v. 405, n. 6787, pp. 704-706.
46. G. Rouhi, M. Epstein, L. Sudak, and W. Herzog, “Modeling bone resorption using mixture theory with chemical reactions,” *J Mech Mater Struct*, 2007, v. 2, n. 6, pp. 1141-1155.
47. H. Bougherara, M.N. Bureau, M. Campbell, A. Vadean, and L. Yahia, “Design of a biomimetic polymer-composite hip prosthesis,” *J Biomed Mater Res A*, 2007 v. 82, n.1, pp. 27-40.